EVALUATION OF THE LIGHTNING PROTECTION SYSTEM AT THE WSR-88D RADAR SITES

Final Report

By Vladislav Mazur, Principal Investigator and Lothar H. Ruhnke, Co-Investigator

May, 2001

National Oceanic and Atmospheric Administration

National Severe Storms Laboratory

Norman, Oklahoma 73069

Final Report

on the Memorandum of Understanding between the WSR-88D Operational Support Facility of the National Weather Service and the NOAA/National Severe Storms Laboratory

1313 Halley Circle, Norman, OK 73069
E mail: mazur@nssl.noaa.gov

Table of Contents

Introduction 5

Task 1: Evaluation of the Different Types of Air Terminal Systems; Computer-Simulation Studies 6
- Summary 6
- Background
- Assumptions in the Computer-Simulation Model 8
- Results of Computer Simulation 12
- Discussion 14
- Recommendations 16
- References 17

Task 2: Impedance and Current Distribution in the Grounding Grid of the WSR-88D Installations 18
- The Earth Systems Analyzer (ESA –1000) and the Measuring Technique 18
- Results of Measurements 21
- Recommendations 24

Task 3: Field Observations of Performance of the WSR-88D Lightning Protection System 26
- Background 26
- Observational Instrumentation and a Setup 27
- Results of Observations 32
- Recommendations 43
- References 43

Task 4: Utilization of Lightning Damage Information for Improvement of WSR-88D Lightning Protection 44
- Background 44
- Solution Based On New Data Flow 45
- Proposed Lightning Reporting Form (Web page) 46

Appendix: Leader Potential and Electric Field Change 48
- Introduction 48

[Table of Contents, contd.]

Measurements 49
Conclusions 51
References 52

Publication and Presentations Related to Work on the MOU 53

Acknowledgements 53

Introduction

The Memorandum of Understanding (MOU) between the WSR-88D Operational Support Facility (OSF) of the National Weather Service, and the National Severe Storms Laboratory (NSSL) established a cooperative program to examine lightning protection at the WSR-88D radar sites. This multi-year agreement, initiated in Fiscal Year 1997-98, ends in Fiscal Year 2000-01. Dr. Vladislav Mazur served as NSSL's Management Point of Contact and Technical Point of Contact for this MOU. Mr. Russell D. Cook served as OSF's Management Point of Contact, with Mr. Patrick Massie as the OSF Technical Point of Contact. Dr. Lothar H. Ruhnke served as a consultant to the project for NSSL.

The objectives of the MOU were a comprehensive evaluation of the performance of the lightning protection system and recommendations for its improvement. Therefore, two major tasks of the MOU became the evaluation of (1) the air terminal system (air terminals and down conductors) of the antenna tower, which is the dominant structure of the radar installations, and (2) the grounding systems at the installations. Identification of the type of lightning damage to an installation is important both for determining the nature of the problem in lightning protection of the installation, and verification of the effectiveness of the suggested remedy to cure the problem. The national network of WSR-88D radars has been built using the same blueprint for lightning protection for all sites. The analysis of lightning damage information obtained from the entire national network may be an effective way for determining a common problem in the lightning protection system. Therefore, another task of the MOU was for NSSL to suggest a method of collecting and evaluating lightning damage information for possible implementation in operational practice.

On the third year of the MOU, it became clear that it is necessary to conduct an experimental validation of the results of computer-simulated modeling of lightning interaction with ground structures at a radar installation under thunderstorm conditions. This became still another new task, of field observation at selected sites with a high probability of lightning damage. This task included synchronized measurements of the essential parameters characterizing cloud-to ground flashes that affect the installation, and lightning-induced effects in the grounding system.

The Final Report is organized into sections that reflect the results and recommendations bearing on the individual tasks of the MOU.

Task 1: Evaluation of Different Types of Air Terminal Systems; Computer-Simulation Studies.

Summary. A three-dimensional computer simulation of the interaction between downward negative stepped leaders of cloud-to-ground lightning and a radar antenna tower was conducted, to determine the dynamics of the attachment process, and their dependence on leader potential, distance to the leader, and type of air terminal (a single vertical rod, a crown of thorns, or the alternative type: lightning diverters). The results of the modeling for negative leaders with an average potential of -40 MV, and a low potential of -10MV suggest that the pattern of interaction between a descending leader and a tower does not depend significantly on the type of protection device. Our modeling results indicated that negative stepped leaders do not noticeably turn toward the grounded structure until one step prior to jump-over to it or its air terminal. This contradicts the conventional interpretation of the dynamics of lightning interaction with a grounded structure as the gradual convergence of a downward and an upward leader toward each other. In cases of powerful lightning (with leader potentials> -40 MV), all types of air terminals would perform equally well; in other words, they would become points of lightning attachment. In cases of weak lightning (with leader potentials of –10 MV or less), the leader either misses the tower completely, or it strikes the structure below the air terminals, depending on the distance between the leader and the tower. In the case of weak lightning, the lightning diverters would perform better than other types of air terminals.

Background

This study was necessitated by the need to find an optimal and cost-effective method of lightning protection for antenna towers of the national network of WSR-88D weather radar stations. The antenna tower is the dominant vertical structure at a radar site; therefore, it is prone to being struck by lightning. Air terminals installed on top of the fiberglass radome are expected to be the preferred attachment points, and to provide the path for lightning current via down-conductors to the ground. A strike to the radar antenna itself, however, may not necessarily constitute an electrical hazard. This is because the mechanical gear and electrical and electronic equipment of the radar antenna is usually enclosed in a well-grounded metal "box."

We were unable to discern with certainty the original purpose for the installations of air terminals on top of radomes, but it seems to be the need to protect the fiberglass radome itself from being damaged by a lightning strike. The radome performs the important function of protecting the radar antenna from wind and other weather elements. There are known cases of radome

sections having been blown off after a lightning strike shredded a fiberglass panel. It is desirable that the air terminals neither attract lightning strikes to the tower, nor allow lightning to attach to the radome. Of further concern is the cost of maintaining the air terminals, because the harsh environment (freezing rain, ice, and wind) at the remote locations of the radar sites causes repairs of the air terminals to be both difficult and expensive.

Traditionally, lightning protection of a radome is accomplished by installing an air terminal (a single vertical lightning rod on the radome's top) with several (usually four) down conductors connected first to the metallic structure of the tower, and then, to the ground (Fig. 1a). Another type of air terminal, called a "crown of thorns" (one vertical at the top and four on the sides), was also implemented on several WSR-88D sites (Fig. 1b). The expectation was that such a scheme would be effective for protecting against lightning strikes on the side of the radome. The crown of thorns, however, has a high maintenance cost, due mostly to icing and strong-wind-related problems.

Inspections of the inner surfaces of radomes at some WSR-88D sites equipped with air terminals of both types have revealed the presence of burn marks. The burn marks indicate points and paths of lightning penetration through the radome (See Fig. 2). The presence of burn marks suggests that lightning may bypass the air terminal to strike, instead, the fiberglass panel on the side of the radome. In view of such evidence, there is a need to examine the effectiveness of the existing types of air terminals in protecting the radome from lightning damage. Understanding the physics of the attachment process to a ground structure may help to explain the reasons for the failure of air terminals, and may help us to design a more effective lightning protection system.

In searching for an alternative scheme of lightning protection for the radomes of WSR-88D radars, we looked at the lightning protection technique for radomes on aircraft that use lightning diverters. Lightning diverters are metallic strips installed either outside or inside the radome, spaced so as to minimize distortion of the radar antenna pattern, and connected at the base to the fuselage (ground), but open at the radome top. In essence, the system of diverters resembles a Faraday cage that provides an electrostatic shield to the interior, but leaves the structure penetrable by electromagnetic waves at radar frequencies (see Fig.1c,d).

We evaluated the performance of different types of lightning air terminals by conducting a three-dimensional computer simulation of the interaction between a downward negative leader and a radar tower. A similar modeling approach was used in [1], to simulate the interaction of the negative stepped leader with a grounded vertical mast.

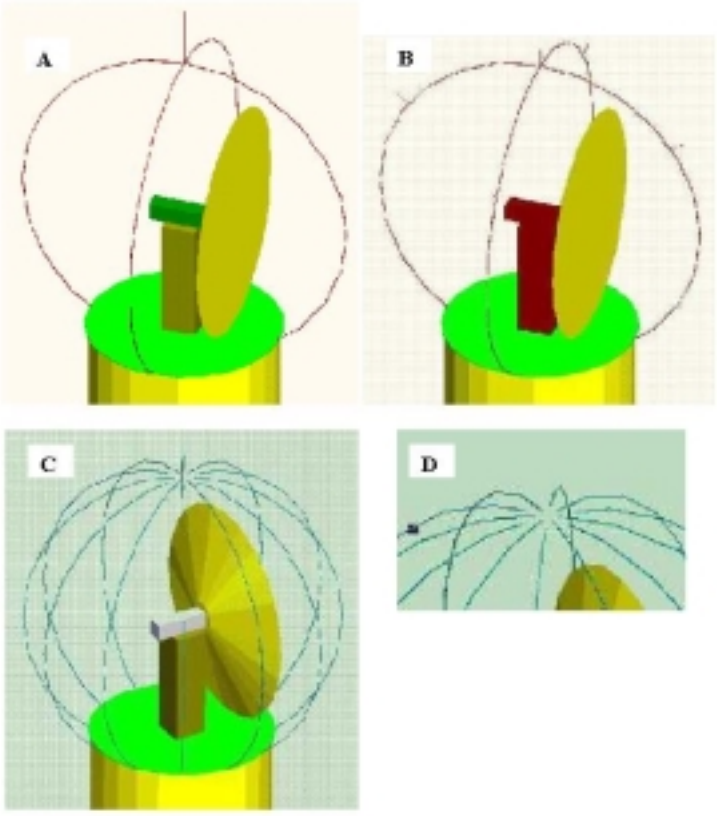

Figure 1. Types of lightning protection air terminals used in our modeling
A -a single vertical rod with four down conductors. B – a "crown of thorns" with four down conductors. C – lightning diverters. D – enlarged view of the top of C.

Assumptions in the Computer-Simulation Model

In the computer simulation, we model in three dimensions both the leader and the structure with their actual dimensions and electrical and material properties (see Fig. 3). We view the results of our modeling to be of a qualitative nature, with the objective of clarifying the process of the interaction between the leader and radome. Numerical solutions were obtained in a space of 280 m (height) x 200 m (length) x 200 m (width). (Note: the limits on the solution volume we have implied for computational purposes of achieving a desirable accuracy of solutions may affect some of the quantitative results obtained.)

We start with a leader that has already advanced from the cloud to about 200m above the ground. At that altitude, the leader is assumed to be vertical. Its diameter is determined from the assumption that the radial electric field in the charge-carrying part cannot exceed 3 MV m^{-1}. The potential of the leader determines the severity of the lightning strike. Moreover, we assume that the leader potential is constant over the length of the leader, as channel conductivity is very high and leader current low, justifying negligible potential drops over the

last 200 m of the leader. We also ignore the influence of the ambient electric field, because it is small compared to the electric field produced by the leader.

Figure 2. Burn marks on the inner surface of the radome of WSR-88D radar.

As the negative leader approaches the ground, growing electric fields on the protruding elements of the structure may lead to the development of upward positive leaders. The selection of a proper value for the propagation velocity of an upward leader, however, presents a challenge for the modeler. There exist no field measurements of an upward leader's velocity during its propagation toward a descending negative leader. Such measurements would be very difficult indeed to obtain. All available references for the velocity of positive leaders are from either studies of sparks in long gaps, rocket-triggered lightning studies, or observations of upward leaders from tall structures [2, 3]. The most quoted values are 10^4 m s^{-1} for the initial stage, with gradual acceleration to 10^5 m s^{-1}. Therefore, we considered two options for the upward positive leader velocities: $5x10^4$ m s^{-1} and $5x10^5$ m s^{-1}. With an average assumed velocity of the downward negative leader of 10^6 m s^{-1}, the ratio of the velocities of the two leaders (hereafter called the speed ratio) would be 20:1 and 2:1, for slow and fast

upward leaders, respectively. For simplicity's sake, the velocities of both leaders were considered to be constant.

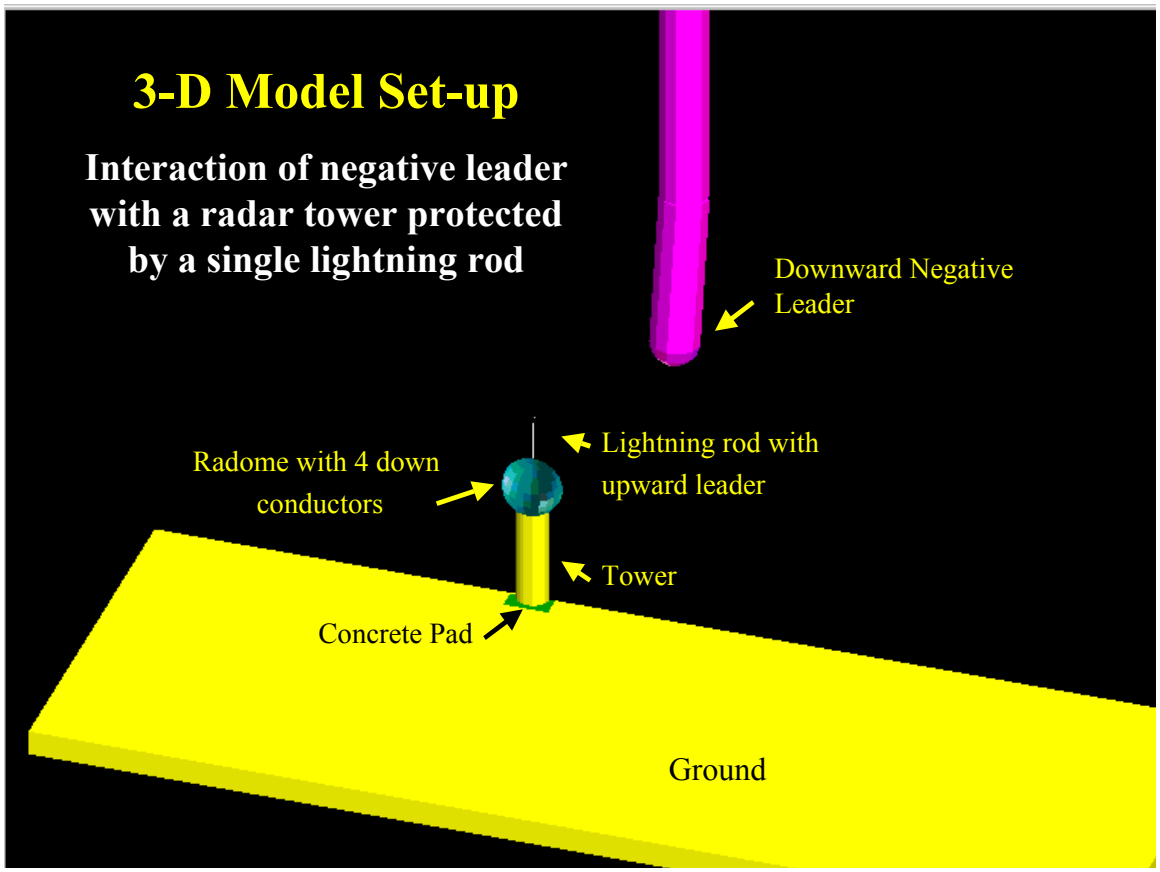

Figure 3. A three-dimensional model of computer simulation of the interaction between a downward negative stepped leader and antenna tower protected with a single lightning rod. Shown is the half of the model that is symmetrical relative to the YZ plane.

There are two conditions to be fulfilled in order for an upward leader to propagate. First, if the upward leader starts from a sharp point on the structure as a glow discharge, it must make the transition into a spark-type discharge. The leader may start from a blunt point-shaped element of the structure as a spark-type discharge without the glow discharge phase. (Unfortunately, because of the scale limitation, we cannot resolve the shape of the structural element in our model to address this issue.) Secondly, the ambient electric field in the vicinity of the starting point must be sufficient to support the sustainable propagation of the leader (the so-called stabilization field). The stabilization electric field, E_{st}, is described in [4] as a function of altitude, ambient pressure and temperature. For the given height, H=30 m, of the radar antenna tower, the stabilization potential $P_{st} = (E_{st} \times H)$ is 2.15 MV. In the model, an upward positive leader starts propagating when the ambient potential reaches this value.

By solving Poisson's equation numerically, we can obtain an electrical potential and electric field at any point in the computational volume. The dynamics of the interaction between two developing leaders (one descending in steps, the other ascending continuously from the ground structure) is reproduced as an incremental development, in stages. Each stage corresponds to one step of the negative leader. The positive leader starts when the negative leader produces an ambient potential near the tip of the lightning rod of P=2.15 MV. The length of the extension for the upward positive leader is a fraction of the step-length of the negative leader, depending on assumed ratios of propagation velocities for the two leaders.

The solution for the three-dimensional potential distribution is analyzed after each stage, in order to determine the direction and length of the next step of the negative leader, as well as the direction of the upward positive leader that advances during the pause between the steps. The procedures used in this analysis are based on the physical model of leader development described in [1]. We determined the direction and length of the leader step by using the following procedure: First, we calculate the length of the corona breakdown region, L_{st}, in the direction of the previous leader step. Then, we find, on a circle with radius, L_{st}, the direction where the potential at the edge of the breakdown region (leader tip) is at its maximum. This would be the direction of the maximum E-field vector at the tip of the leader. (This direction is assumed to be the direction of the next step of the leader.) Finally, we determine the magnitude of L in a new direction, which would be the length of the next step.

In the first set of modeling conditions, the distance between the axis of the downward negative leader and the axis of symmetry of the antenna tower was 30 m, which is also approximately the height of the top of the radome above the ground. We conducted modeling with two values of negative leader potential, -40 MV and –10 MV. The first value is considered to be an average potential (the maximum can be > 100 MV), while the second value represents the low end of the potential range. We also considered two ratios of propagation speed for the downward and upward leaders: (1) a scenario of a slow upward leader, with a speed ratio of 20:1, and (2) a scenario of a fast upward leader, with a speed ratio of 2:1.

To investigate the effect of distance on the interaction of weak leaders (potential of -10MV) with a ground structure, we considered a second set of modeling conditions, with distance between the axis of the downward negative leader and the axis of the antenna tower of 15 m, well within the so-called "cone of protection."

Results of Computer Simulation

The modeling results for a negative leader with –40MV potential (its vertical axis 30 m away from the tower, and the speed ratio of the two leaders at 20:1) are the following:

1. For all three types of lightning protection (single rod, crown of thorns, and diverters) the output of the interaction is the same; specifically, the negative leader strikes the rod, a thorn, or the radome (presumably a lightning diverter). The progression of the downward leader is illustrated in the composition of superimposed images from individual steps in Figure 4, for the case of a single vertical rod, and in Figure 5, for the case of diverters, as types of lightning protection.
2. An upward leader starts from a single lightning rod earlier than from a crown of thorns. This is expected, because a single vertical rod is much taller than a vertical thorn. No upward leader starts from the diverters protecting the radome in the alternative scheme of protection, because they have no vertically protruding parts.
3. In all three cases, negative leaders react to the presence of the tower by starting to turn toward it just one step before the final jump-over to the radome.

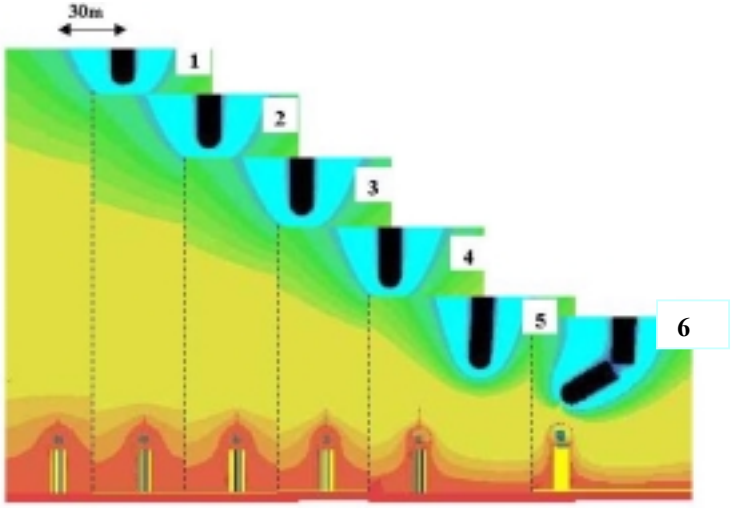

Figure 4. Progression of a negative stepped leader of –40 MV potential towards a radome protected with a single vertical rod (superimposition of potential distribution plots in YZ plane). In steps 1-3 of the negative leader (30.5m; 30m; 30.5m long, respectively), the simultaneous development of both the upward positive and downward negative leaders occurred straight vertically, until the negative leader reached a height of 129 m (step 3). The upward positive leader propagated continuously, by ~ 1.5 m per each step of the negative leader. At step 4, the upward leader turned 1.5 ^{0} toward the negative leader. Then at step 5, the negative leader turned 3.2^0 and the upward leader turned 10.2 ^{0} towards each other. Step 6 is the jump-over toward the radome, with a step of 38 m long.

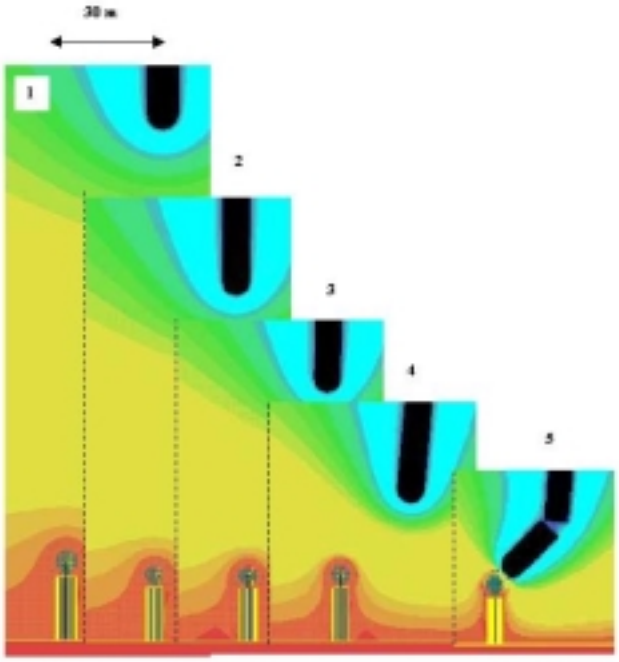

Figure 5. Progression of a negative stepped leader of –40 MV potential towards a radome protected by lightning diverters. The negative leader descended straight toward the ground until it reached the height of 127 m (step 2). In the absence of sharp points on the radome, no upward leaders were expected to occur. With steps 3 and 4 (each of 35 m and 41 m long, respectively), the negative leader turned gradually toward the tower (step 3, 1.7^0; step 4, additional 3.1^0), and then jumped over to the tower during the last step 5 of ~ 50 m length.

Modeling results show that increasing the speed of the upward leader (by using the speed ratio 2:1) does not change its reaction toward the descending negative leader. As in the case of a slow upward leader (with a speed ratio of 20:1), it turns toward the negative leader one step earlier than the negative leader turns toward the upward leader. The character of the interaction between descending negative and ascending positive leaders does not change with the increasing propagation speed of the upward leader, except for the height at which the jump-over takes place. As anticipated, this height is greater in the case of the faster upward leader.

Summarizing the results of modeling for a negative leader with a potential of –10MV, approaching the tower just outside its cone of protection (~30 m in our case), we found the following: In all cases, and seemingly independent of the speed ratio, the interaction between the leader and the tower was the same, specifically, the negative leader reacted to the presence of the tower by turning gradually towards it, prior to passing the tower and going to ground (Fig. 6).

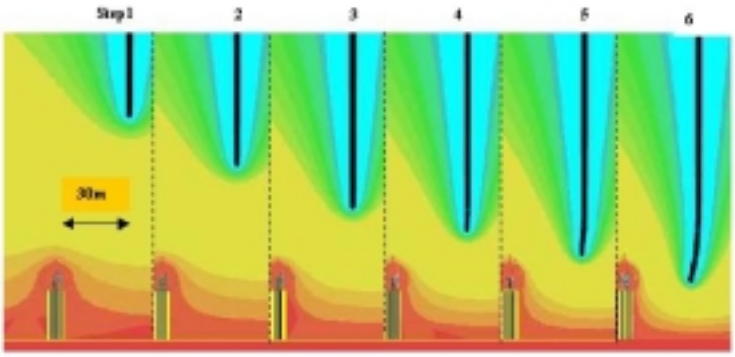

Figure 6. Progression of a downward leader of –10 MV potential towards a radome protected by a single vertical lightning rod. The negative leader propagated straight down until it reached the height of 53 m above the ground at step 3, when conditions for the development of the upward leader were met. At step 4 (9.2 m long), the negative leader turned 1.5^0 toward the antenna tower, and the upward leader made a first advance of 45 cm long, straight upward. At step 5 (9.8 m long), the negative leader turned an additional 4^0 and descended below the height of the tip of the lightning rod, while the upward leader from the rod advanced an additional 50 cm, turning 15^0 toward the negative leader. At step 6 (10.5 m long), the negative leader turned an additional 6.3^0 towards the tower, while the upward leader turned an additional 10^0 toward the leader. After step 4, the leaders had already missed each other, and the negative leader went to ground.

The purpose for modeling the case of a negative leader with –10MV potential descending 15 m away from the tower was to find out how the negative leader would interact with a radome when descending to ground within the volume of cone protection, i. e., closer than 30 m. Once again, the interaction of the leader with the tower had the same pattern for both types of protection devices: the negative leader did not intercept the upward leader, but struck the radome instead (see Fig. 7). We believe that the case of a weak leader at close range to the tower reproduces the situation that occurs when lightning strikes the side of a radome, with burn marks visible on the inner surface of the radome (see Fig. 2).

Discussion

Results of the modeling for negative leaders with potentials of average (-40 MV) and low (-10MV) values suggest that the pattern of interaction between a descending leader and a tower protected by three different types of lightning protection schemes does not depend significantly on the type of protection device. We cannot exclude the possibility that, in those cases of leaders that produce strikes to a side of the radome, which have low potential values and which are at close range to a tower, the crown of thorns may be more effective than a single vertical lightning rod. In cases of powerful lightning, with leaders of great potential values, both the single rod and crown-of-thorns types of air

terminals would perform equally well; in other words, they would become points of lightning attachment. The results of our modeling confirm the observations and inferences made in [5], that "striking distance is not a constant size, as once thought, but it is a function of the intensity of the lightning strike. Thus, for a weak stroke, the attractive effect may be too small to prevent a strike to a point close to a conductor, or even to a point below the tip of a vertical lightning rod." So, the challenge is to select the type of air terminal that achieves better performance in protecting the radome from lightning flashes with low leader potentials, as well as one that will have minimum maintenance problems and cost.

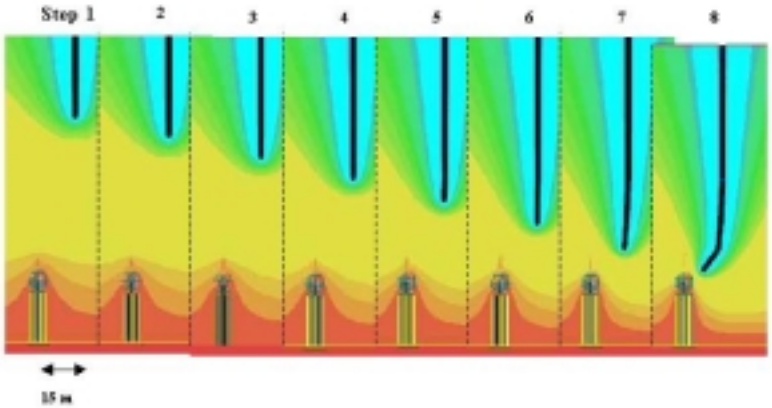

Figure 7. Progression of a negative stepped leader (15 m away from the tower horizontally) towards a radome protected with a single vertical rod. A stabilization potential to support a sustainable propagation of the upward positive leader was reached after step 1. At steps 2 and 3, both leaders moved straight vertically, with increments of 8 m and 0.4 m, respectively. The upward leader started to turn towards the downward negative leader at steps 4 through 8 by 1.7^0, 1.2^0, 5.3^0, 15^0, and 41^0 angles, respectively. The negative leader turned toward the upward positive leader starting at steps 5 through 8 by 1.9, 0.0, 5.0, 29^0 angles, respectively. The negative leader did not intercept the upward leader, but struck the radome instead.

The alternative type of radome protection, with lightning diverters, does not react to the descending lightning leader by starting an upward leader when the leader passes nearby. This feature can be of great benefit under certain conditions, e.g., when the radar site is located at high altitude. At altitudes of several hundred meters ASL, an upward leader can start from a protruding air terminal under the ambient electric field of a thundercloud which equals, or exceeds, the stabilization field. Such leaders can turn into cloud-to-ground flashes that strike the tower; they would not, however, occur without the air terminal. A similar situation might occur in winter storms, even with a radar tower at sea level (e.g., the seacoast of Japan). In winter thunderstorms, with a cloud base only a few hundreds meters above ground, the ambient electric field is usually much stronger than that in summer thunderstorms, and may exceed the value of the stabilization field. In that case, lightning protection using

diverters is more effective than the other two types of air terminals. Lightning diverters require very little maintenance, because wind and ice do not affect them. The number of diverter strips that can be installed without interference with the radar antenna pattern is greater that four (the usual number of down conductors for the single-rod or crown-of-thorns type air terminals). Therefore, in the case of lightning strikes to a side of the radome, the diverters will serve as effective down conductors.

The question of upward leader velocity change in response to descending downward leaders remains unresolved. It is reasonable to anticipate an acceleration of both leaders toward each other, with a sharp increase of electric field in the gap between them. However, we can take some comfort in the observations in [5], "that the lengths of the upward streamers from open ground or from low structures are fairly short, and that the pronounced kinks below which the lightning channel goes straight to the point struck lie usually only moderately higher." These observations suggest that upward leaders are slow (perhaps ~10^4 m s^{-1}), and that they do not have enough time to accelerate before being intercepted or passed by the downward leader.

The conventional interpretation of the dynamics of lightning interaction with a grounded structure sees it as a gradual convergence of the downward and upward leaders towards each other. Our modeling results suggest that this picture should be corrected, at least for structures of low heights. Negative stepped leaders do not turn significantly toward the grounded structure until one step prior to jump-over to the structure or its air terminal. So, the pronounced kinks in the visible pattern referred to in [5] are likely to be the starting points of the final step of the downward leader.

Recommendations

The type of lightning protection examined in our modeling, i.e., one that uses metallic diverters, may provide an effective alternative to air terminals with a single vertical rod or a crown of thorns in protecting radomes from lightning with a wide range of leader potentials, both weak and powerful. Lightning diverters require minimum maintenance under harsh environmental conditions, as opposed to air terminals that are susceptible to breakage by strong winds and icing. Lightning diverters work quite well on aircraft, and there is no reason that they should not be equally effective in protecting the radomes of ground-based radars.

In view of the unreliability of air terminals to protect a radar site against weak lightning flashes with low leader potentials, the additional measures of lightning protection for radar equipment shelters, like grounded metal masts at or near the four corners of the radar site, may be effective. If a weak lightning flash misses the antenna tower, it would most likely attach to one of these metal masts. For weak lightning flashes, the height of the mast (it should be taller than the shelter,

but shorter than the antenna tower) and its positioning may be determined by taking into consideration both the dimensions of the radar site and the range of the leader's step length near the ground.

We have emphasized the importance of leader potential in our modeling of the interaction between downward and upward leaders, and its role in determining the lengths of the steps in negative leaders to ground. Our approach differs from the traditional one in the literature, which considers either the charges on the leader or the return stroke current as lightning parameters for determining the "striking distance" for grounded structures. In the Appendix to this report, we have introduced a new method of obtaining magnitudes of leader potential from field measurements of electric field changes produced by cloud-to-ground flashes.

References

[1] Mazur, V, L. H. Ruhnke, A. Bondiou-Clergerie, and P. Lalande, Computer simulation of a downward negative stepped leader and its interaction with a ground structure, J. Geophys. Res.,105, 22,361-22369, 2000.

[2] Kito, Y., K. Horii, Y. Higashiyama, and K. Nakamura, Optical aspects of winter lightning discharges triggered by the rocket-wire technique in Hokuriku district of Japan, J. Geophys. Res., 90, 6147-6157, 1985.

[3] Yokoyama. S, A. Asakawa, K. Miyake, T. Shindo, T. Wakai, and T. Sakai, Leader and return stroke velocity measurements using Advance Measuring System on Progressing Feature of Lightning Discharge (ALPS), 25th International Conference on Lightning Protecrion, Rhodes-Greece, 18-22 September 2000.

[4] Lalande, P., A. Bondiou-Clergerie, G. Bacchiega, I. Gallimberti, Theoretical analysis of the conditions for stable propagation of a positive leader, Submitted to J. Geophys. Res.

[5] Golde, R. H., Lightning (Vol. 2, Lightning Protection), Academic Press, New York, 1977.

Task 2. Impedance and Current Distribution in the Grounding Grid of the WSR-88D Installations

Presently, the components of the grounding grid of the lightning protection systems at WSR-88D facilities are characterized and tested by measuring only the bonding resistance and resistance-to-earth, both of which are DC resistances. Lightning, however, is a transient event, with strong high-frequency components in its current. In order to evaluate the effect of lightning current flow through a grounding system, the impedance of the system should be measured or estimated. To date, this practice has not been implemented. As a consequence, the behavior of a grounding system cannot be realistically evaluated for the possibility of side flashes, arcing and sparking when the facility is struck by lightning. NSSL conducted an evaluation of impedance and resistance of the grounding systems at selected WSR-88D installations, using a new technique and a recently developed instrument for impedance measurements, the Earth System Analyzer (ESA-1000).

The Earth Systems Analyzer (ESA -1000) and the Measuring Technique

The Earth Systems Analyzer (ESA-1000) depicted in Fig. 8 is a portable, microprocessor-controlled instrument that allows us to measure DC resistance, as well as the impulse impedance of a grounding system. Here, briefly, is the concept of impedance measurement utilized by the ESA-1000.

Figure 8. The ESA-1000, ready for measurements of the impulse impedance of a grounding point at a leg of the antenna tower.

The instrument generates an injection current pulse, which has a waveform that simulates the waveform of a lightning return stroke current (not in amplitude, but in rise and decay times). We found for the current waveform:

$$I = I_0 (\exp(-t/T_1) - \exp(-t/T_2))$$

The time constants are T_1 = 100 μs and T_2 = 2 μs, and the amplitude of the injected current I_0 varies from 3 to 10 A, depending on soil resistance between the injection point and a test electrode. The "impulse impedance" Z_p , shown on the measuring instrument, is the ratio of the peak voltage drop over the grounding network to the peak current injected. Although this impedance is not true impedance in electrical engineering terms (a true impedance is frequency dependent), it reflects the grounding system's performance under transient conditions, and is relatively simple to measure. Knowing the peak lightning current, we will know the peak voltage between the grounding system of the installation and the outside ground.

The grounding system of a WSR-88D site is a grid of interconnected grounding rods (see Fig. 9). When we measured DC resistance at various grounding points, the instrument indicated a total ground DC resistance of the entire grid on the order of 0.1 ohm (the typical value for all inspected sites). In order to test effectively the DC resistance or the impedance of an individual grounding rod in this multi-electrode system, it is necessary to disconnect the rod from the rest of the grid. By doing this, we would eliminate the effects of parallel ground paths from the measurements of the local ground. For transient lightning currents, each grounding rod in the interconnected grid has a somewhat different impedance to the ground, because only the elements of the grid in the immediate proximity of the rod, rather than the entire grid, have a significant influence on the performance of this grounding point. Therefore, some points on the grounding grid will not carry any lightning current of that injected to an antenna tower. One of the objectives of a measurement program, then, is to also find out which grounding points are carrying lightning currents and which do not. In view of the fact that the disconnecting of individual grounding rods from the grid of a WSR-88D installation is not achievable, the interpretation of impedance measurements represents a challenge.

In employing the ESA-1000, our main concern was the accuracy of the measurements and their reproducibility. We found that the lead lines from electrode E of the ESA-1000 to a grounding point add a potentially significant error to the measurement, because of the lead lines' own impedance (a fact which is, unfortunately, not reflected in the ESA-1000 manual). The impedance of the lead lines, measured separately, showed the approximate values for the short and long lead line at Zsl=9.6 ohm and Zll=46.5 ohm, respectively. A true grounding impedance measurement, therefore, is obtained after subtraction of the impedance of the lead line used from the values indicated by the instrument.

We implemented this approach at several radar sites. Later, we minimized the error caused by the lead line by shortening the length of the lead line from the instrument to the grounding point to one inch.

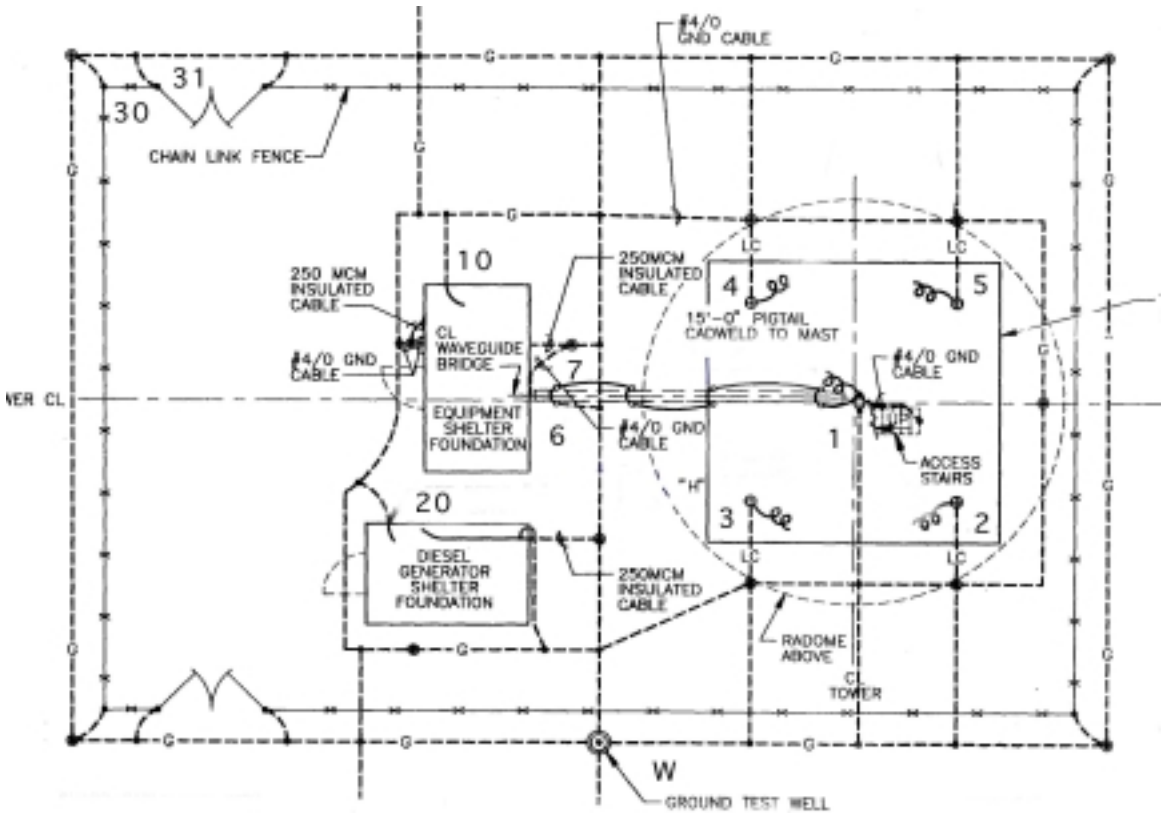

Figure 9. Diagram of the grounding grid at the typical WSR-88D radar installation. Grounding points 1-7 are at the antenna tower and the waveguide bridge; points starting with 10 are at the equipment shelter; points starting with 20 are at the generator shelter; points starting with 30 are at the fence; and the point marked W is at the test well.

Of further concern was the effect of the dimension of the grounding grid on impedance measurements. The three-point method we used with the ESA-1000 requires two independent grounding points, one for current injection and another for potential measurements. At WSR-88D installations, with a grounding grid that covers a substantial area and is adjacent to commercial land, it is rather difficult to position grounding points at distances from the grid much farther than the dimensions of the grid, and also without close proximity to underground metal pipes or cables. The effect of the grid dimensions when the test electrode is not far from it is to decrease the potential difference between the voltage test electrode and the grounding rod of the grid, and thus to underrate the actual impedance value measured by the instrument. We believe that we were unable to fully eliminate this negative effect of the grid dimensions on the impedance measurements conducted.

We conducted impedance measurements with the ESA-1000 for grounding systems at sites in Norman, OK, Oklahoma City, OK, Las Vegas, NV, Melbourne, FL, Key West, FL, Ruskin, FL, and Albuquerque, NM. In the course of these measurements, we developed a better understanding of the limits and possibilities of the ESA-1000. We present in this report detailed results for two sites: in Ruskin, FL, surveyed in the summer of 2000, and in Norman, OK, surveyed in the spring of 1999.

Results of Measurements

The radar antenna tower is the dominant tall structure at each radar installation and, therefore, the most probable structure to which a cloud-to-ground lightning flash would attach. This is the reason why the impedance measurements at each site were made at the following accessible grounding points (see Fig. 9): at the central grounding point of the tower (#1), at the four down conductors at each of the four tower legs (#2-5), and at the two grounding points of the waveguide bridge adjacent to the tower(#6, 7). Only for one site, in Ruskin, FL, did we make additional measurements at a high point on the tower, under the assumption that this would represent the grounding impedance of the entire tower.

The ESA-1000 instrument provides the ability to trace the path of transient signals as they travel through the structure into the ground. This feature of the instrument allows us to determine the distribution of lightning currents from the top of the tower (a probable point of lightning attachment) through its grounding points. The procedure consists of injecting a current pulse of known magnitude into a point of possible impact and measuring (recording) the amplitude of current pulses at different grounding points with a current clamp and a ScopeMeter. Not all current paths were accessible, as the current clamp available has a maximum diameter for the conductor of one inch, and some portion of the total current flows into the ground via the steel structure, rather than through the intended down conductors. The results of measurements of impulse impedance and current distribution among the grounding points of the antenna tower at two sites, in Ruskin, FL and Norman, OK, are presented in tables 1 and 2.

The waveforms of the current pulse injected into the tower and of the current pulses at the grounding points of the Norman site are shown in Fig. 10. Measurements at the grounding points, besides points 1-5 in Ruskin (table 1) and points 1-7 in Norman (table 2), produced no detectable current pulse above the noise level. The numbers in tables 1 and 2 indicate that the current injected into the antenna tower dissipates to the ground mainly through the grounding points of the tower. In the case of the Ruskin tower, two grounding points at the waveguide bridge (#6, 7) carried no current to the ground, while at the Norman site, the same grounding points did carry current.

Table 1. Impulse impedance and current pulse distribution at the WSR-88D in Ruskin, FL

Location/Point #	Impedance Zi (ohm)	% of the injected current
Tower Top	5	100.0
1	3.1	13.3
2	4.2	21.4
3	2.8	12.2
4	4.2	13.1
5	7.6	6.4
Sum on points 1-5		**66.4**
Not accounted		**33.6**

Table 2. Impulse impedance and current pulse distribution at the WSR-88D in Norman, OK

Location/Point #	Impedance Zi (ohm)	% of the injected current
Tower Top	not measured	100.0
1	14.4	14.6
2	10.4	17.1
3	10.7	4.9
4	11.4	6.1
5	9.4	15.0
6	12.2	2.8
7	14.9	3.3
Sum on points 1-7		**63.8**
Not accounted		**36.2**

The fact that we accounted for only 66.4% and 63.8% of the injected current in Ruskin and Norman, respectively, is explained by the following: At both WSR-88D sites, in addition to the grounding cables at each leg of the tower, the antenna tower footing anchor bolts are connected with #4/0 GND cable to the bottom outermost reinforcement bar of the concrete foundation (see Fig. 11). The additional conducting path to the ground from the tower through the footing anchor bolts accounts for the remaining 33.6% and 36.2% of the injected current at the Ruskin and Norman sites, respectively. Similar results were obtained at the Albuquerque site, where the total current through the seven grounding points associated with the antenna tower carried 79.6% of the injected current. The exception was the site in Oklahoma City, where the total current through the five main grounding points was 92.2% of the total injected current. We found, however, that the antenna tower footing anchor bolts at the Oklahoma City site were not connected to the bottom outermost reinforcement bar of the concrete foundation, and thus to the grounding grid, as they were at all other sites.

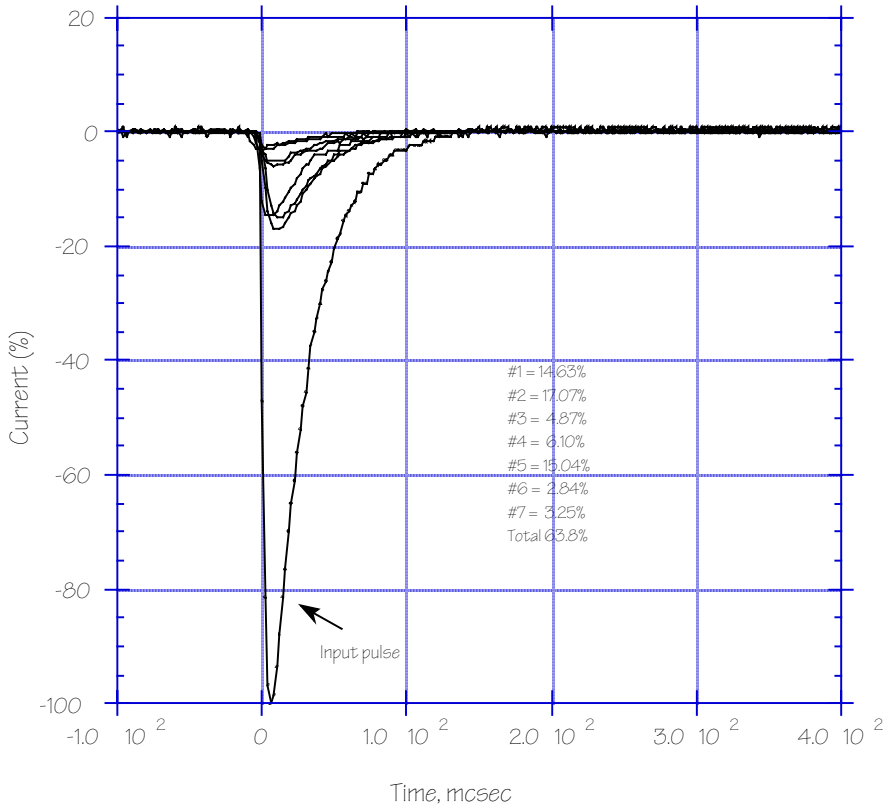

Figure 10. Current waveforms at the grounding points of the Norman site.

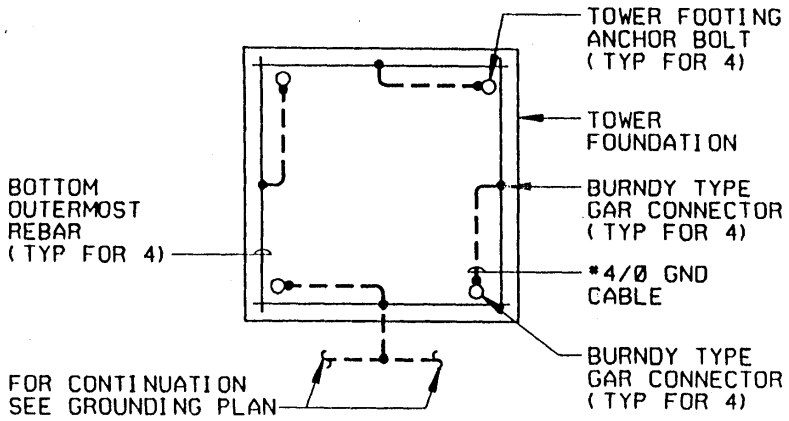

Figure 11. Detail of the drawing showing connection of the footing anchor bolts of the antenna tower to the reinforcement bar of the concrete foundation and then to the grounding grid.

If we had been able to measure the impulse impedance at the grounding points of the tower by disconnecting them from the grounding grid, we would have obtained the impedance values that, when multiplied by the current

flowing through the point to the ground, produce the voltage at the injection point of the current pulse. (This voltage value would have been the same when calculated for the currents and impedance at different grounding points of the tower.)

However, these measurements could not be made for the interconnected grounding grid of the WSR-88D sites. What we actually measured as the impulse impedance at each grounding point includes the impedance of the tower structure itself, in addition to the impedance of the part of the grid near the grounding point. As a result, the impedance values obtained at all points are all different, but basically are all on the same order of magnitude (see Tables 1, 2).

The average value of impedance at five points of the tower at the Ruskin site is 4.4 ohm, close to the impedance measured at the tower itself, i.e., 5.0 ohm. We believe, in the case of an interconnected grounding grid, the averaging of impedance values measured at the grounding points (which carry the current) is a reasonable way to estimate the impedance of the tower's grounding system. Using this approach, the average impedance of the tower's grounding system is 12 ohm for the Norman, OK site, 29 ohm for the Oklahoma City, OK site, and 28 ohm for the Albuquerque, NM site.

At some installations, lightning hazards to the weather forecast building can be and, indeed are, caused by a tall communications tower close to the building. This situation exists at the Ruskin, FL site. Impedance measurements on the communication tower there showed a value of 5.2 ohm for grounding impedance, which is of an acceptable value.

Our conclusion, based on the measurements presented above, is that the antenna towers at Ruskin, FL and Norman, OK are well grounded. The grounding systems at Oklahoma City, OK and Albuquerque, NM have higher impulse impedance, most likely because of the higher resistivity of the soil there that affects the DC resistance component of the impulse impedance.

We believe that the combining of multi-point measurements of impulse impedance and current distribution is the most reasonable and best way to characterize the performance of the grounding grid in response to lightning transient currents.

A validation of our measurements of antenna tower grounding impedance can be found in field observations of current to ground and loop voltages during upward leader development from the tower induced by nearby lightning flashes. (See results of Task 3).

Recommendations

It should be obvious that using DC resistance measurements for evaluating of the performance a grounding system is misleading; impulse impedance measurements produced a more realistic picture of the actual state of a grounding system. For sites where DC resistance of the grid showed 0.1 ohm

(e.g., the Oklahoma City site), impulse impedance was hundreds of times higher than DC resistance.

Based on the measurements of impulse impedance conducted, we believe that the present "blueprint approach" to designing the grounding systems at all WSR-88D sites is not justifiable, because of the natural differences in soil conditions and soil conductivity at the various sites. Specific measures for decreasing impedance at a site with poor soil conductivity should be considered.

Although we cannot endorse any particular instruments for impedance measurements, in the course of this project we have demonstrated the utility of an approach based on these measurements.

Task 3: Field Observations of Performance of the WSR-88D Lightning Protection System.

Background

In order to validate the assumptions and results of computer-simulated modeling of lightning interaction with an antenna tower, the attempt was made to compare them with field observations at a radar installation under thunderstorm conditions. This task requires synchronized measurements of currents/voltages at one or more points of the grounding grid and a surface electric field change produced by lightning to correlate a phase of lightning flash with a lightning-induced effect in the grounding system. Multiple video observations of lightning in the vicinity of the site, and, if possible, video observation of induced upward leaders from the structure would serve to verify a direct or nearby lightning strike to an installation. The reality of natural lightning activity suggests that field observations could require more than one storm season of lightning measurements at the same radar site. Measurements of current and voltages on the grounding grid could also validate estimates of the ground impedance (see Task 2), which was not a straightforward, but rather a complex task.

The first attempt to conduct field observations was made during the summer 1999 at the Las Vegas WSR-88D site, located at the summit of the dominant mountain peak (height 3250 ft ASL), southwest of Las Vegas. This site was selected because of numerous cases of lightning damage to the installation. The field observations at Las Vegas did not yield meaningful results, mostly due to difficulties in maintaining and monitoring the instruments installed. Remote access to the instruments was not available, and physical access to the site was rather limited because of its location. However, we, monitored cloud-to-ground flashes in the vicinity of the site using the National Lightning Detection Network (NLDN) data, but did not register any direct lightning strikes to the installation during the entire 1999-thunderstorm season.

During the Summer 2000 thunderstorm season, we conducted a second attempt at video monitoring of cloud-to-ground lightning activity synchronized with electrical measurements of lightning flashes, as well as measurements of lightning-induced effects in the grounding system. The radar site selected for these observations was the WSR-88D installation in Ruskin, FL. The Tampa Bay area, where this site is located, has the highest density of cloud-to-ground (CG) lightning in the United States. Additional advantages of making observations at this site were the easy physical access to the site, and available communication lines for the remote monitoring of PC status and data files.

An additional objective of video monitoring of lightning activity in the vicinity of the selected radar site was to verify direct lightning strikes to the

installation, either to the radome of the antenna tower, or to the two radio towers located at the side of the weather forecast office building.

Observational Instrumentation and a Set-up

The video monitoring system (Fig. 12) consisted of three components: (1) an "all-sky" system with a conical mirror and a conventional video camera viewing the mirror from above (this system is effective in recording luminous channels to ground); (2) a video camera viewing the radome and the air terminal at its top; and (3) a video camera viewing the tops of two radio towers. The video monitoring system was connected via a fiberoptic link to a device where video images from the three cameras were multiplexed and recorded at slow speed on a time-lapse VCR, with a GPS time stamp superimposed on one view. All video cameras were powered at all times, but recording was controlled by a triggering device that reacted to a certain high magnitude of the ambient electric field (this due to the presence of electrified clouds above).

Measurements taken of electric field changes near the ground at low frequencies allow us to evaluate the intensity of CG flashes, as well as the number and characteristics of return strokes in these flashes. An electrostatic sensor (called a "slow antenna") is connected to a buffer amplifier, and the output signal is then fed to a multi-channel A/D converter of a PC. The records are stored for later analysis on hard disk. The A/D converter we used had a time resolution of 200 μs, which was sufficient to distinguish cloud-to-ground from intracloud flashes, and to determine the amplitudes of return strokes. A GPS time stamp attached to each data file allowed us to identify the same flash measured simultaneously at other locations with other sensors, and to identify a CG flash recorded by the NLDN that determines the location of the CG flash with an accuracy of approximately +/- 500 meters, and which estimates the maximum current to ground in each flash.

While we were measuring the responses of the grounding system to incoming leaders of CG flashes, we were also interested in estimating the characteristics of these leaders. The potential of the lightning leader is the one variable crucial in deriving the main characteristics of the leader process, such as leader charges, channel diameter, and charge per unit length. The leader's potential is also the dominant factor affecting leader interaction with a ground structure, including the maximum length of the final "jump-over" toward the structure, as demonstrated in [Mazur et. al., 2000], with a computer-simulated modeling of leader interaction with a tall mast. In the course of our work on this MOU, we developed a method of deriving the leader potential from measurements of electric field changes produced by cloud-to-ground flashes. (A description of this method and initial results are presented in the Appendix.) Previously, leader potential values have only been estimated empirically. During the summer of 2000, we made the first set of measurements with a multiple system of "slow

antennas" to determine the magnitude of potentials for downward negative stepped leaders.

Figure 12. Setting up the video surveillance system at the WSR-88D site in Ruskin, FL, Summer 2000.

Calibration of the slow antenna system produced a ratio of 150 V/m of the ambient electric field to 1 V at the input of the buffer amplifier. (This ratio did not change more than +/- 8% for the flashes investigated.)

Although the probability of a direct strike to an installation is low, a very close lightning flash may induce upward-propagating leaders from the air terminal of a radar tower. The electrical measurements on the grounding system may provide valuable information on currents and waveforms of these upward leaders.

As part of the grounding impedance measurements with the Earth System Analyzer (ESA-1000), we determined the distribution of lightning currents among the grounding rods of the antenna tower after injecting a simulated lightning current into the top of the tower. We found that the five grounding points (four legs of the tower and one central rod) accounted for the majority of the injected current. Measurements with the simulated current source for the tower in Ruskin, FL showed that 13.1% of the current injected into the tower flows via leg #4 to the ground (see Table 2). A clamped current probe (see Fig. 13) with a sensitivity of 1 mV/A at leg #4 was connected to channel 2 of the A/D

converter. The total lightning current to the radar tower is then equal to the current value at leg #4 multiplied by 8.

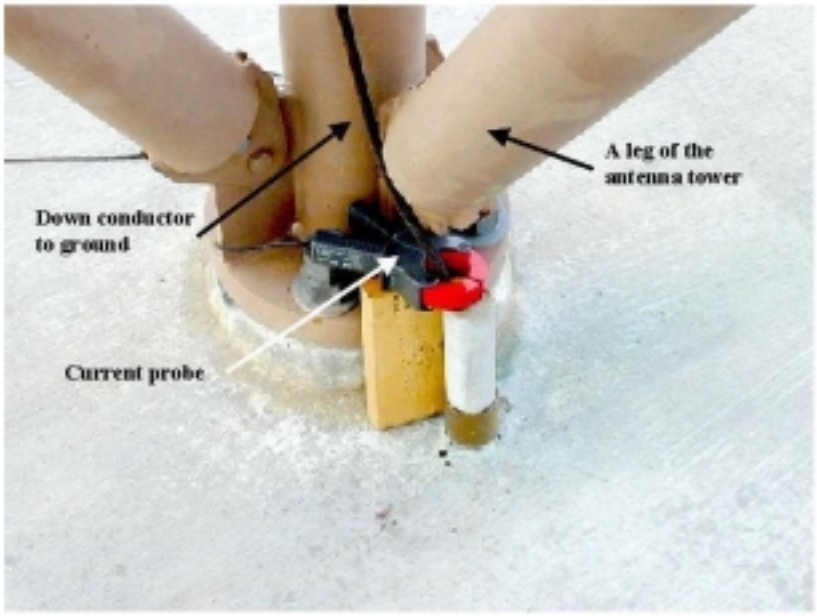

Figure 13. Clamp current probe on a down conductor of an antenna tower leg.

We also measured the "loop voltage" between the ground grid of the installation and an independent ground that would not be affected by a lightning strike to the installation. We could not position the point of the independent ground sufficiently far from the installation to avoid totally the effect of the grounding grid; therefore, the loop voltages measured are not as high as they might be.

Assuming a ground resistance R and an inductive impedance ωL of the grounding grid, then the largest voltage U induced in any single loop (loop voltage) at the installation by a lightning current I is:

$$U = I * (R + \omega L)$$

This is the voltage induced by a lightning strike to the tower, between the instrument ground at the installation and any line coming to the installation and grounded at an outside independent ground (such as incoming power lines, telecommunication lines, water pipes, etc.). This loop voltage usually produces the largest damage to any installation hit by lightning. In our setup, we measured the voltage between the installation's grounding grid and a ground rod outside the radar site. A high voltage 1,000 MΩ resistor was connected between the outside (independent) ground rod (see Fig. 14) and channel 3 of the A/D converter. A 10 kΩ resistor at the input of channel 3, together with the 1,000

MΩ resistor, constitutes a voltage divider. Thus, each 1 V at the A/D converter input is indicative of 100 kV of the loop voltage. The diagram with instrumental setup for conducting the measurements is shown in Fig. 15.

The data recording on a PC was triggered by an electric field change (from the slow antenna system) produced by a lightning flash. The measuring equipment operated autonomously, with remote access to the PC data files via a modem.

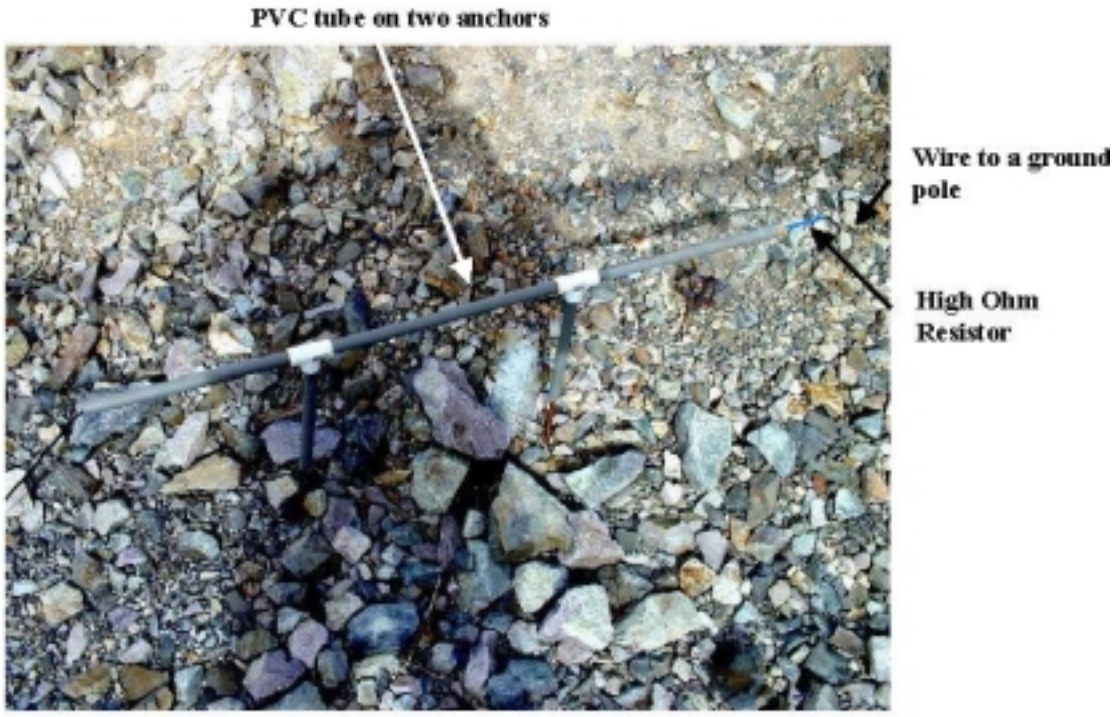

Figure 14: A "loop voltage" probe at the independent ground outside the radar installation.

We also monitored thunderstorm activity in the vicinity of the radar site by downloading daily data from the NLDN for the previous 24-hour period. This had a dual purpose: (1) to verify data acquisition at the site, and (2) to collect statistical data about CG flash density near the site. During the Summer 2000 thunderstorm season from June 25 to October 8, there were 54 days with thunderstorms within 20 km from WSR-88D site at Ruskin, FL, with the two most active periods being from the middle of July to the beginning of August, and then from the end of August to the middle of September (see Fig. 16). The plot of the number of flashes within 20 km from the site during each thunderstorm day in Fig. 17 shows that up to 1300 flashes may occur in such an area during a single storm day. An example of ground flash mapping within a 20X20 km area for one storm day is shown in Fig. 18.

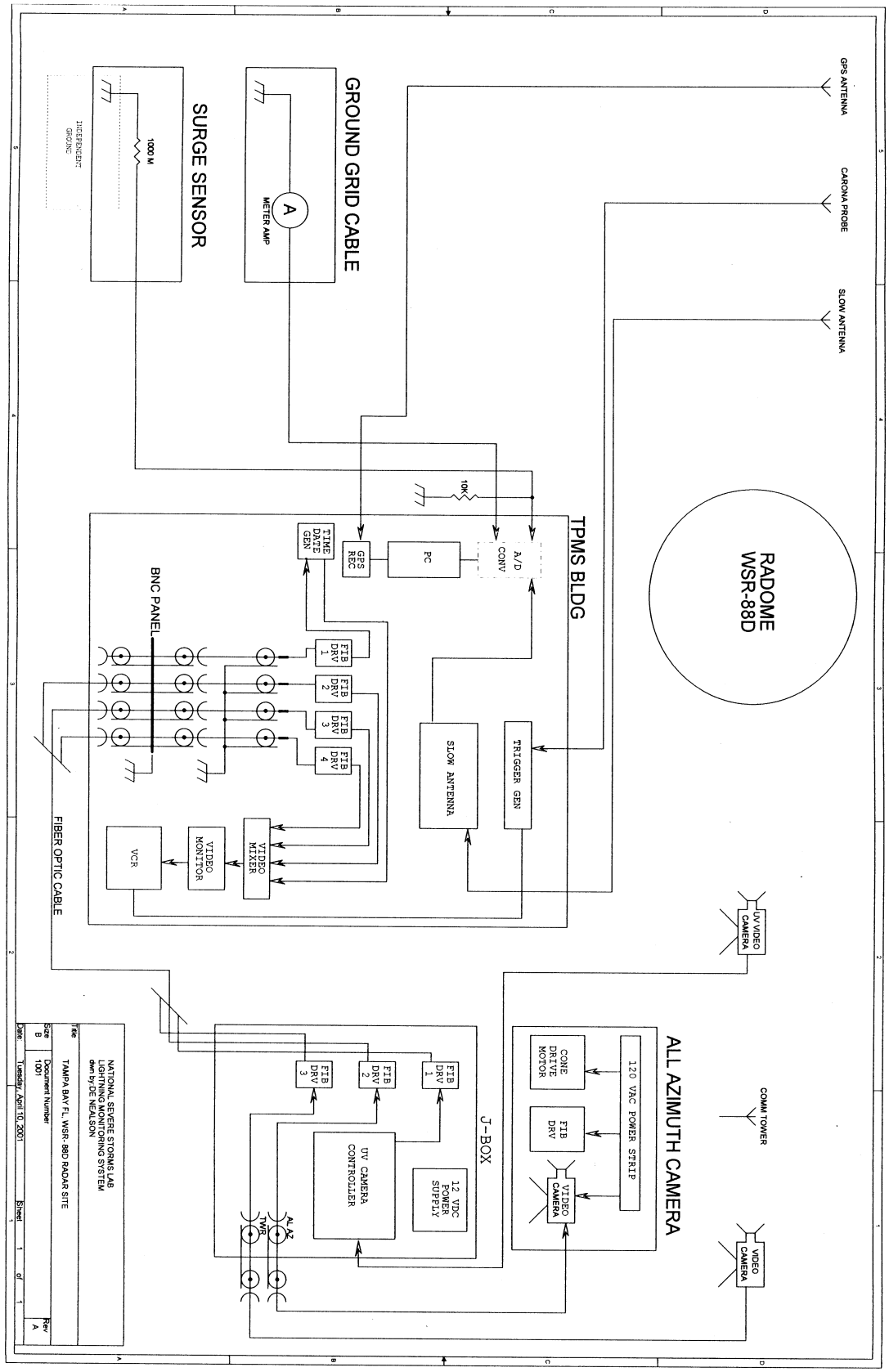

Figure 15. Diagram of instrumental set-up at the WSR-88D site in Ruskin, FL.

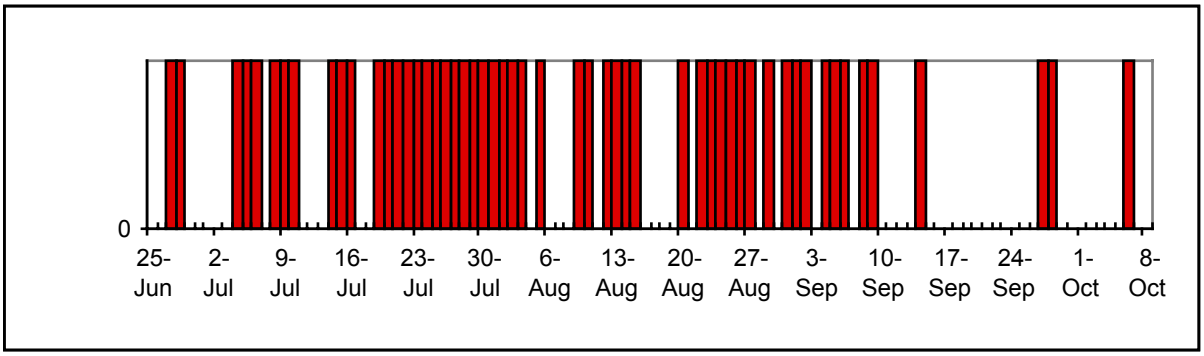

Figure 16. Days with thunderstorms within 20 km of the WSE-88D site in Ruskin, FL, during the Summer 2000 storm season.

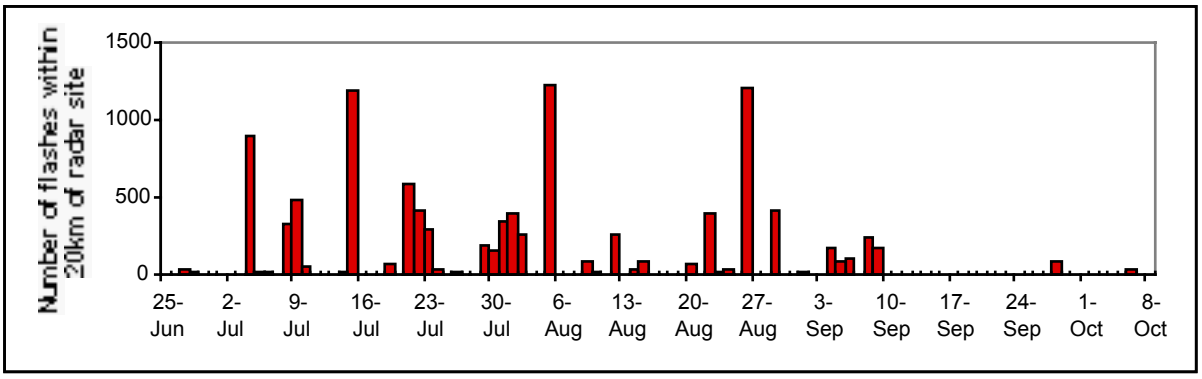

Figure17. Number of flashes within 20 km from the radar site during each thunderstorm day during the Summer 2000 storm season.

Results of Observations

During the entire summer 2000-thunderstorm season, there were no direct lightning strikes to the radar installation. According to NLDN data, however, there were 22 CG flashes closer than 1 km from the site (see Table 1). Many of these flashes were confirmed with our video monitoring system (a malfunction in the video system occurred after August 27, so video data were lost at the end of the storm season). Figures 19 and 20 show examples of video images of nearby lightning strikes. We were not able to observe with our video monitoring system any upward leaders from the vertical air terminal, possibly because of distance, ambient light, and the frequency band of the video camera.

During several of the nearby CG flashes, we recorded current pulses in the down conductor at leg #4 of the antenna tower, and loop voltage pulses that corresponded to the times of downward negative leaders in multistroke CG flashes. The records for the flash on July 4 at 23:34:28 UT are presented in Figs. 21-23.

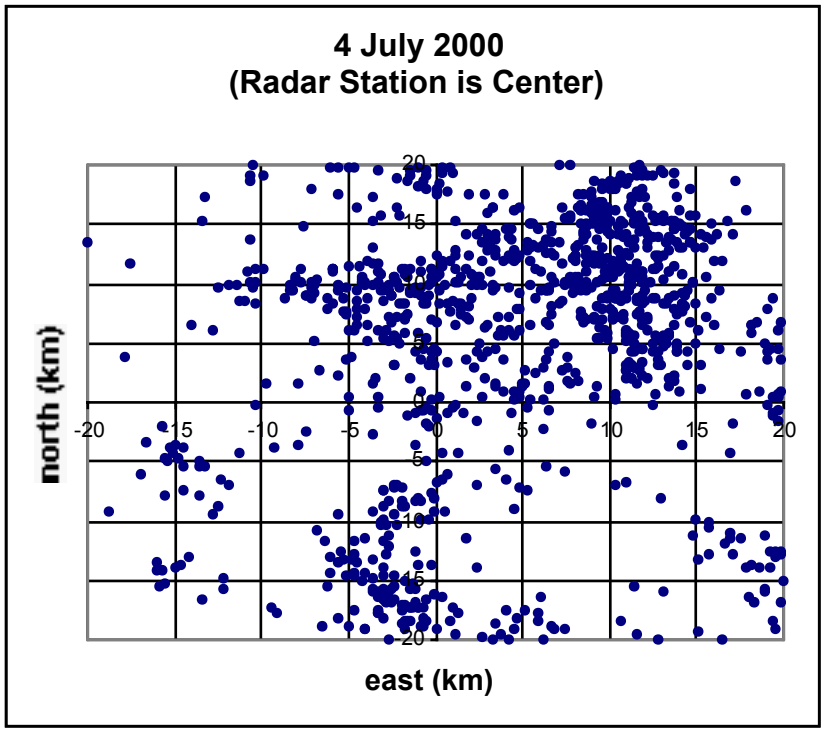

Figure 18. Plot of locations of cloud-to-ground flashes within 20 km from WSR-88D during the storm on July 4, 2000 (902 total flashes in the area)

Table 1. Cloud-to-ground flashes closer than 1 km from the WSR-88D site in Ruskin, FL, Summer 2000.

Date	UT time	D (m)	Date	UT time	D (m)
4-July	23:33:07	723	5-Aug	3:18:05	460
	23:34:28	598	12-Aug	8:51:25	850
	23:34:29	991	26-Aug	23:28:20	613
	23:41:08	204	29-Aug	2:22:10	834
	23:41:08	480	5-Sep	16:18:10	820
8-Jul	15:36:57	696	8-Sep	23:36:08	602
15-Jul	13:34:14	473		23:36:26	777
19-Jul	0:41:20	734		23:36:40	714
	0:52:09	719		23:37:21	709
1-Aug	19:08:37	457	28-Sep	4:08:45	810
	19:08:39	883			
	19:38:37	367			

After an analysis of the timing of the current and voltage pulses in relation to the leader-return stroke sequence in the multistroke CG flash on July 4 at 23:34:28 UT, we found that each current and voltage pulse occurred during the

leader phase of the cycle, rather than during the return stroke phase (see Figs. 24 -28). This means that the current pulses were produced by upward leaders from the antenna tower (most likely from the vertical air terminal), in response to descending negative leaders nearby.

The largest current pulse was induced during the downward leader prior to the fourth return stroke; its estimated value is 5.2 kA. (This value was obtained by dividing the current at leg #4, measured with the current probe, by the portion of the total current flowing through this point to the ground, from the current distribution measurements, i.e., 13%) The fact that the voltage pulses are not proportional to the current pulses is indicative of different waveforms, and therefore, a different frequency composition of the current pulses in upward leaders. The largest loop voltage value of 32 kV occurred during the first leader. This loop voltage was probably handled well by the surge suppression circuit, and therefore did not produce damage to the installation.

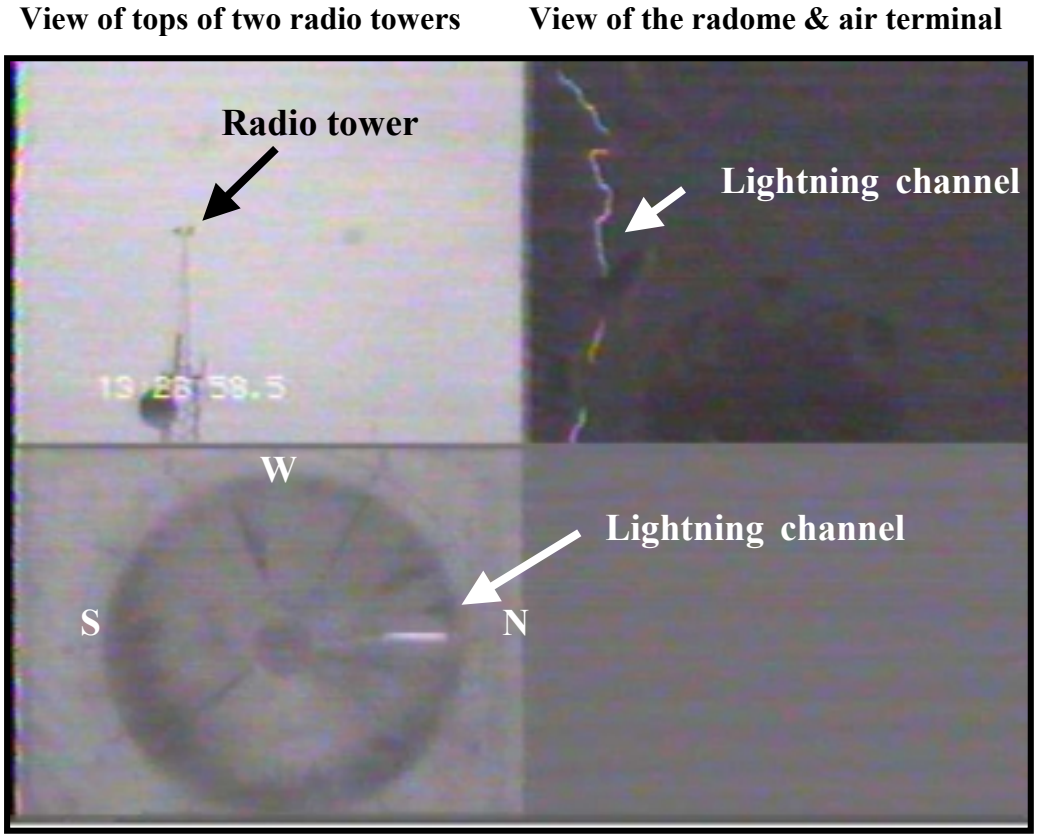

Figure 19. Composite views of the video monitoring system at the WSR-88D site in Ruskin, FL. A channel to ground of a nearby lightning flash is seen in two of three activated quadrants.

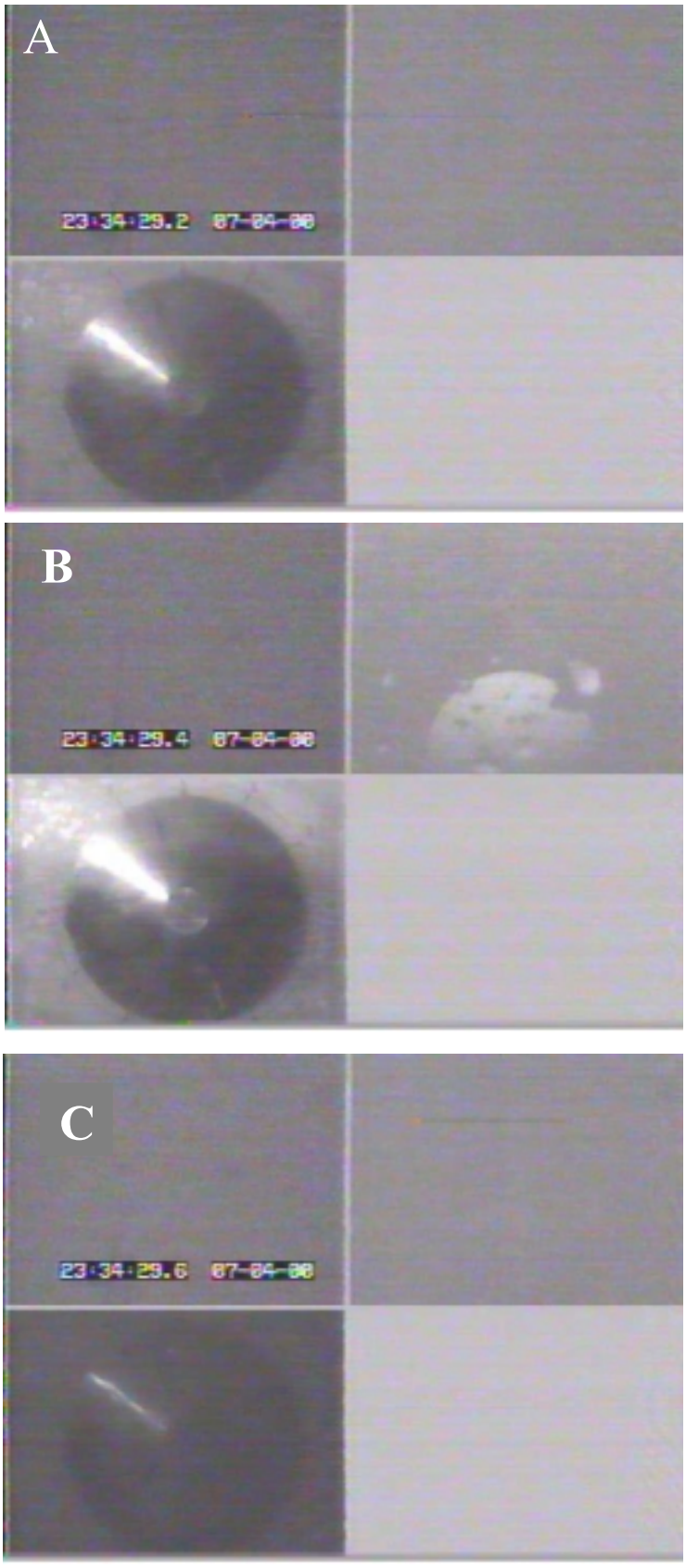

Figure 20. Video images of the multistroke cloud-to-ground flash at 23:34:29 UT, July 4, 2000, less than 1 km from the radar site. Views A, B, and C show images of at least 3 return strokes of the 8-stroke flash.

In the CG flash analyzed, the current pulses of the upward leaders we measured ranged in amplitude from 400 A to 5.2 kA; the loop voltages ranged from 3 kV to 32 kV. These values may be underestimated, however, considering the somewhat low sampling rate of our A/D converter.

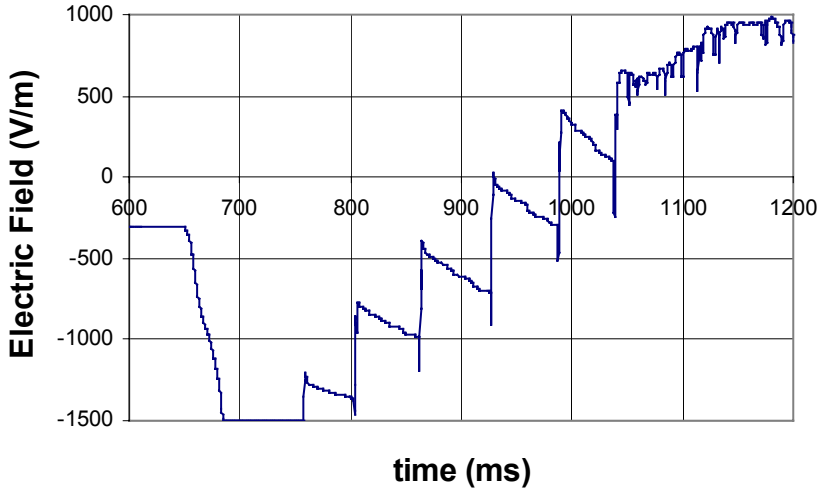

Figure 21. Electric field changes during the CG flash on July 4, 2000 at 23:34:28 UT with 8 return strokes (three return strokes at the beginning of the flash are not seen, due to signal saturation). Vertical axis indicates the ambient electric field values.

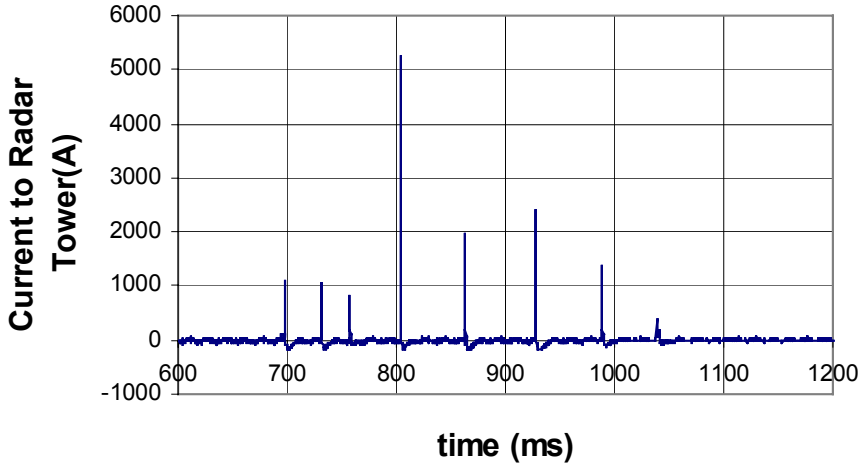

Figure 22. Current flowing through the tower during the flash, from measurements with a probe on antenna leg #4. The eight current pulses correspond to the eight return strokes.

By dividing the loop voltages by the corresponding current pulse values of upward leaders during each cycle of the negative leader-return stroke, we obtain ground impedances of 36.4, 2.0, 6.2, 2.1, 2.2, 2.4, 2.8, and 8.8 ohm for each of the eight upward leaders, respectively. These values vary because of the different frequency composition for each upward leader current pulse, but are mainly in

the range of the impedance measured for the antenna tower in Ruskin, FL (see Task 2)

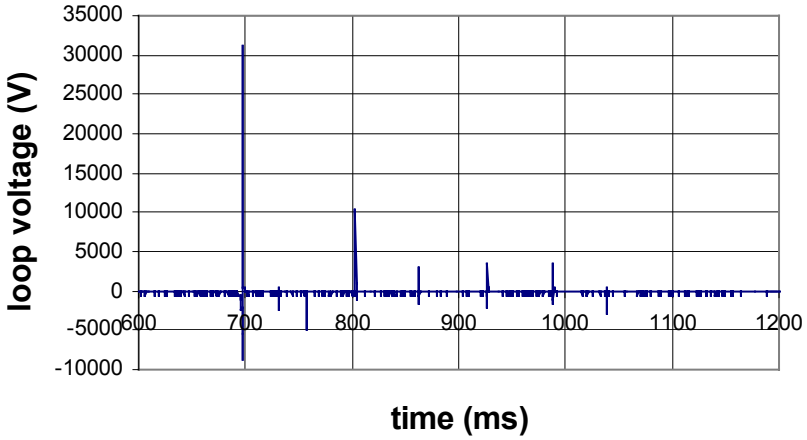

Figure 23. Loop voltages during the flash. The eight voltage pulses correspond to the eight return strokes.

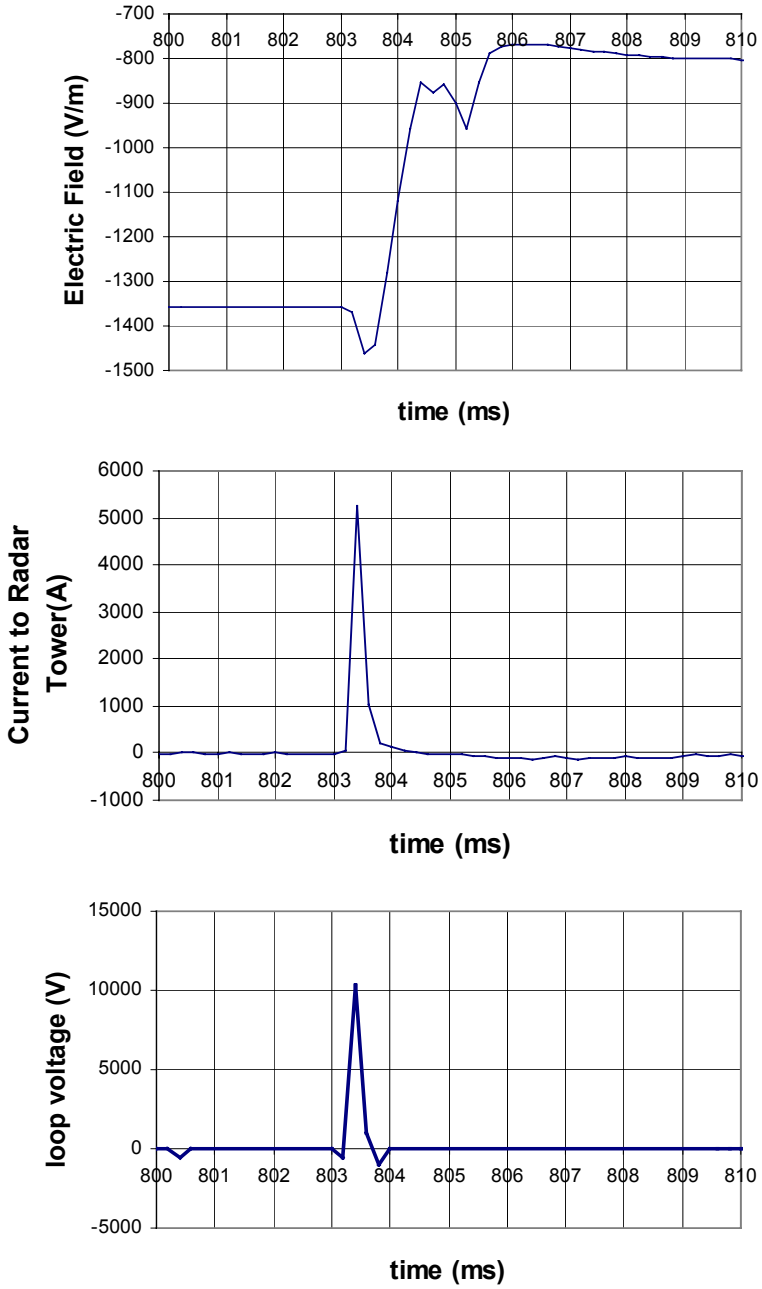

Figure 24. Waveforms of the electric field changes of the fourth leader-return stroke, the current pulse of the upward leader from the tower, and the loop voltage. Notice that the peaks of the pulses occur during the leader stage that corresponds to the decreasing electric field (the increasing field change is from a return stroke).

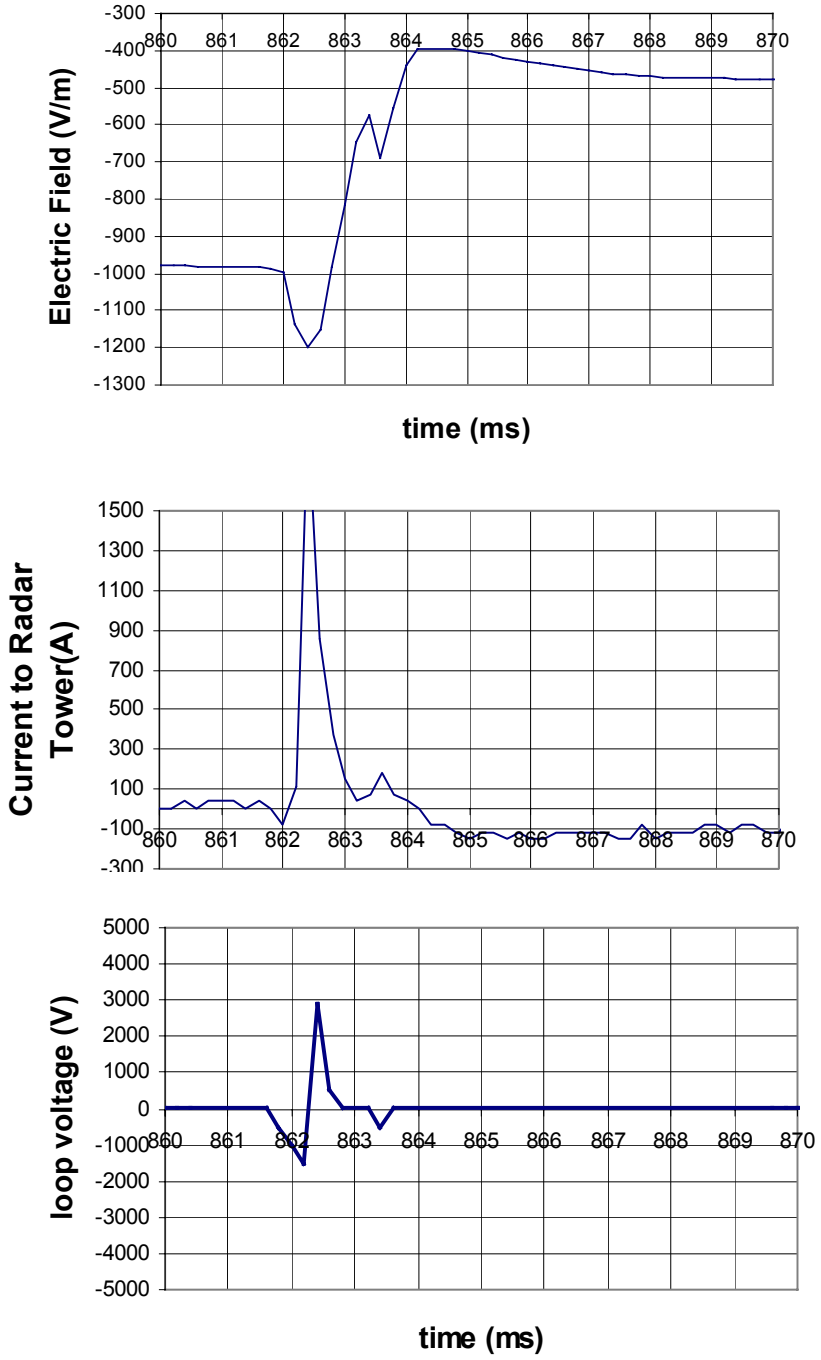

Figure 25. The same as in Fig. 24, but for the fifth sequence of the leader–return stroke.

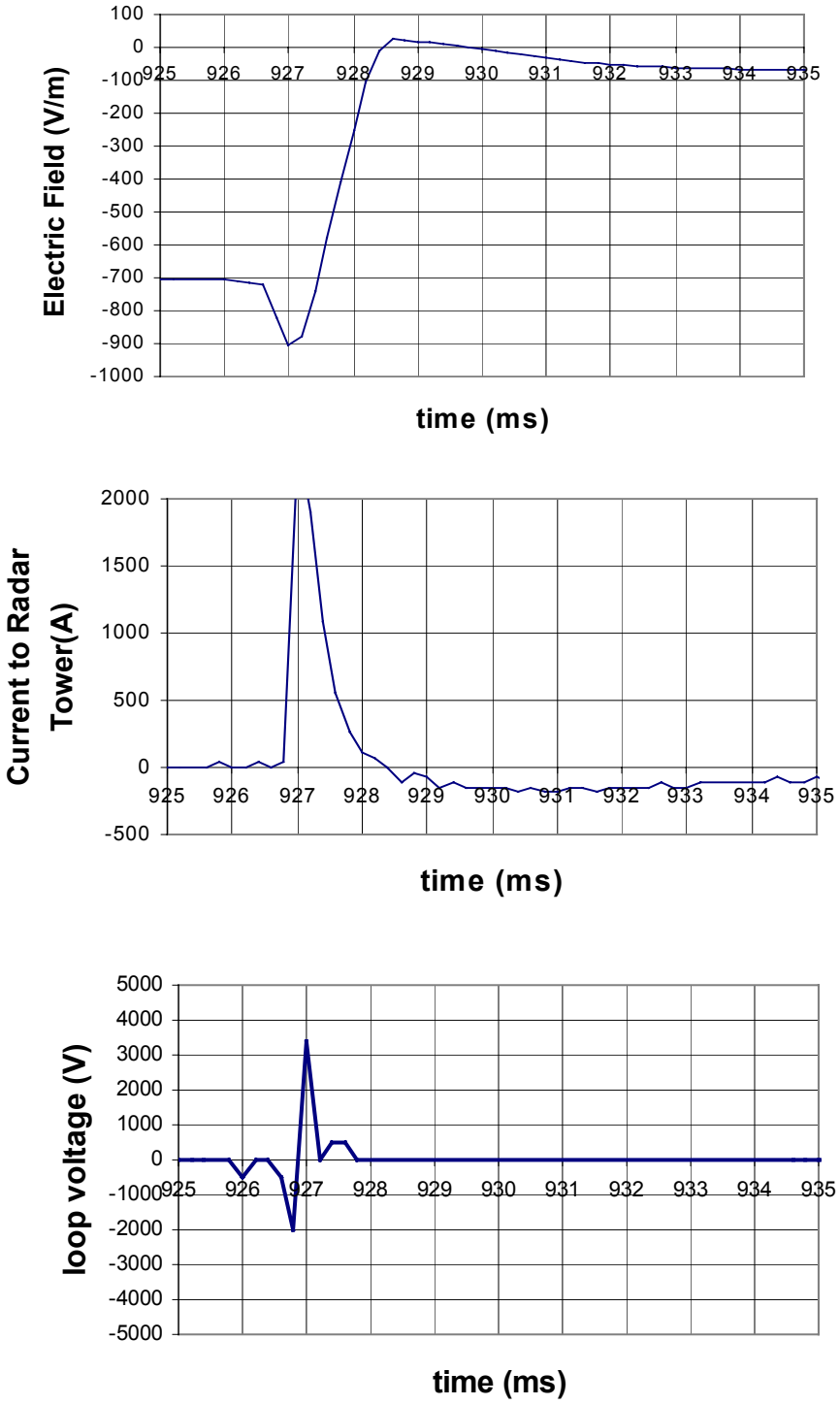

Figure 26. The same as in Fig. 24, but for the sixth sequence of the leader–return stroke.

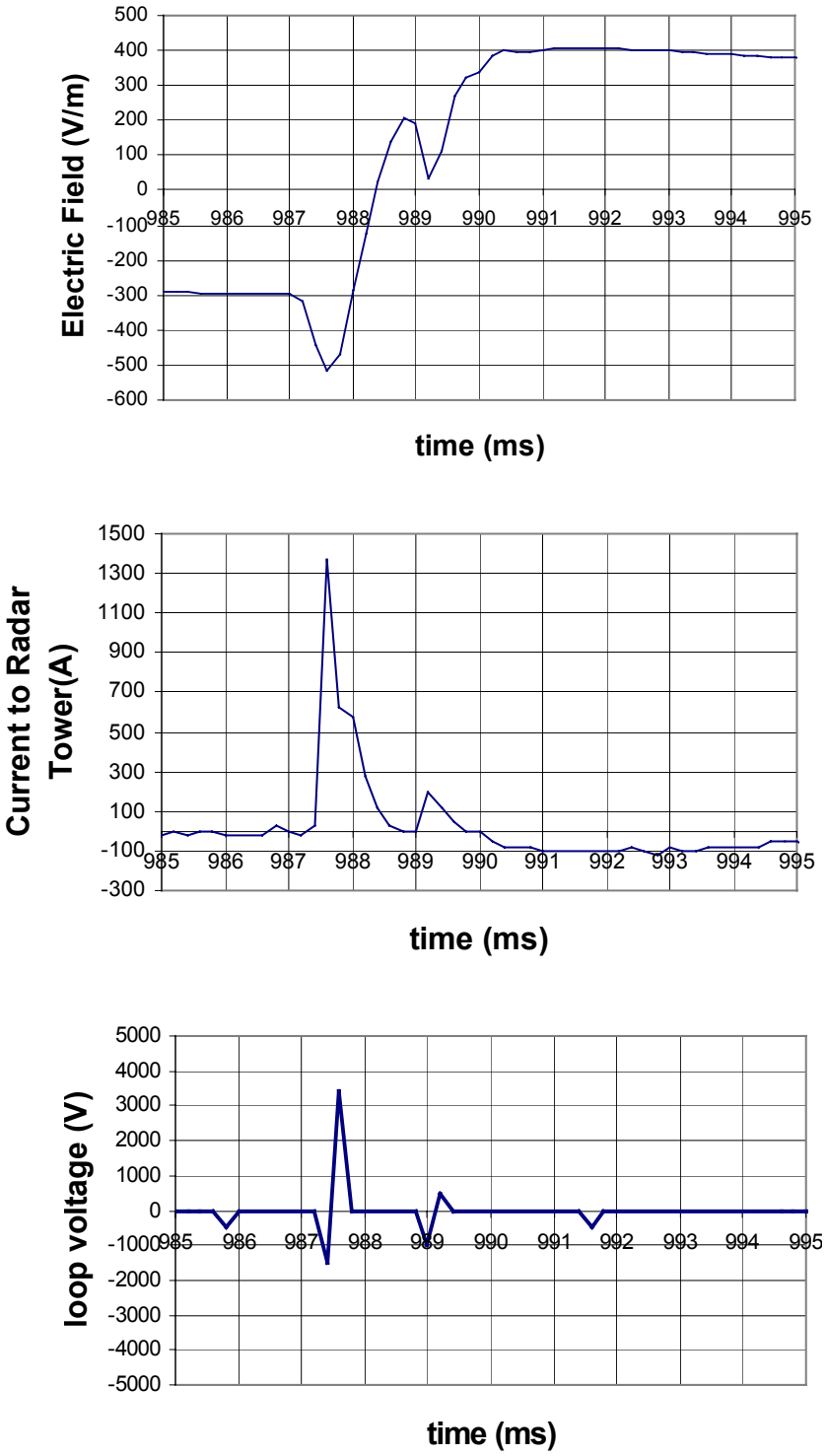

Figure 27. The same as in Fig. 24, but for the seventh sequence of the leader–return stroke.

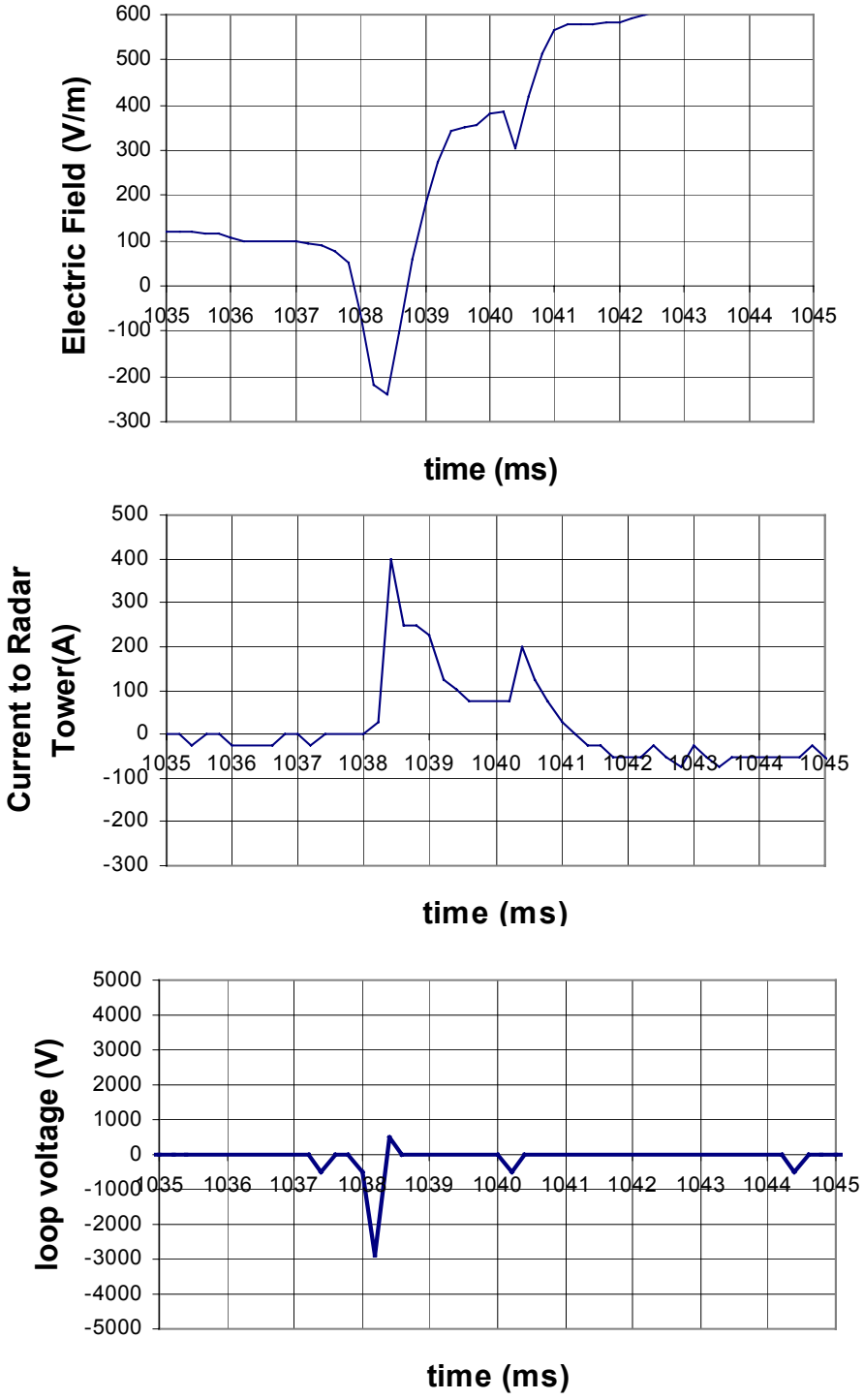

Figure 28. The same as in Fig. 24, but for the eighth sequence of the leader–return stroke.

Recommendations

The system we employed in Ruskin for monitoring lightning-induced effects on the grounding grid of the installation (excluding video monitoring), seems to be a relatively inexpensive and effective way to establish the relationship between lightning characteristics and lightning damage to an installation. Our system may be recommended for selected radar sites that are exposed to lightning hazards, either because of their geographical location, the topography of the site (mountaintops), or unfavorable grounding conditions.

Data from NLDN on timing and locations of CG flashes can be used for the purpose of verification of lightning-induced damage to a radar site and discriminating them from damage by other causes. These data may be easily tailored to a small area around a radar installation, and collected routinely during a thunderstorm season. With relatively small efforts, this information may be gathered for the entire national network of WSR-88 radars.

References

Mazur, V., and L. H. Ruhnke, Computer simulation of a downward negative stepped leader and its interaction with a ground structure, J. Geophys. Res., 105, 22,361-22,369, 2000.

Task 4. Utilization of Lightning Damage Information for Improvement of WSR-88D Lightning Protection.

This task in the MOU between NSSL and OSF addresses the gathering and utilization of all available and obtainable information for determining the problems with the lightning protection system at the WSR-88D sites. The objective of the task is to design a specific procedure for gathering information of interest to OSF and other potential users about lightning strikes to WSR-88D sites. This procedure should require no greater effort than that currently used by electronic technicians (ET) in reporting lightning damage, and should allow for easy access to all information by potential users.

Background

Currently, there are three agencies to whom WSR-88D sites report about lightning related failures and damage: (1) the Engineering Management Reporting System (EMRS) at the NWS Office of Systems Operations, (2) the National Reconditioning Center (NRC), and (3) the OSF WSR-88D Technical Support Hotline, which also provides technical assistance.

The EMRS reporting system utilizes a database with a user interface, and is reachable by dial-in or remote log-in over the Internet, with the user entering information about his site and the failure that has occurred. The function of EMRS is to provide parts failure information, workload effects, and the types of maintenance procedures and actions taken to remedy the failure. Lightning is one of the 15 possible reasons for failure listed in the EMRS codes. The EMRS reporting Form A-26 contains no specific questions or information useful to OSF for determining the specific cause of the lightning damage, or even for verification that damage to the system was, indeed, lightning-related. As a result, the EMRS report has a limited application to the OSF objectives.

The NRC receives information from field sites via paperwork that accompanies the components of the WSR-88D system that failed and should be serviced. The data form has a short space for a description of the cause of the failure. However, there is no requirement in the NRC data form to answer specific questions, which must be addressed, in order to benefit a lightning-damage-cause study by OSF. As a result, the NRC reports have a rather limited application for OSF objectives.

The OSF Hotline is a technical support facility available for field personnel via telephone. The purpose of the Hotline is to provide technical assistance in cases of failures in the WSR-88D system. It is strictly optional for the technicians at the field sites to call the Hotline. However, even if they do call the Hotline, some significant details about the lightning damage may be missed unless the Hotline personnel ask pointed questions.

Our conclusion, after reviewing the present failure-reporting system, is that this system is fragmented, somewhat redundant, overly laborious, and fails to provide complete lightning damage information suitable for the analysis of the integrity of the WSR-88D lightning protection system. Present measures do provide useful data on the damaged components, but do not contain sufficient information for OSF to conduct a lightning-damage study.

Solution Based on New Data Flow

Our proposed solution intends to consolidate all information relevant to the description of lightning damage into a single form available at a Website. This "mother" form will include questions of interest to OSF, NRC, and EMRS, and also will automatically generate subsidiary forms, e.g., the present EMRS A-26 form, and the report forms for NRC and OSF. The Website may be accessed on the local Weather Forecast Office (WFO) computer. The subsidiary reports will go directly to EMRS and NRC. The entire Website form will be available to any user, but OSF or a dedicated vendor will provide the analysis of lightning damage.

This proposed solution would require the cooperation of both EMRS and NRC in changing the current procedures. Design of the proposed Website can be done with OSF's guidance. In designing the Website, consideration may be given to the utilization of the NLDN data to "raise a flag" when strikes occur near a WSR-88D site. Appropriate software may be designed to monitor and record the locations and times of cloud-to ground flashes in a limited area around the sites (see example in Task 3) from the NLDN data base.

Proposed Lightning Reporting Form (Web page)

The purpose of this Web page is to provide a single comprehensive questionnaire which covers all aspects of lightning strike occurrence to a given WSR-88D site, and which describes the damage to the facility produced by, or associated with, a lightning strike. This Web page will be used primarily by OSF or a designated vendor for analysis of the performance of the lightning protection system. Subsidiary reports will be generated by this Website in the formats required by EMRS and NRC, respectively, and will address technical aspects of lightning damage/replacement of components. These secondary reports will be posted for EMRS and NRC[1].

1. Name of the WSR-88D installation[2].

2. Date of the damage occurrence.

3. Time of damage in UT time.

4. Functional area where damage occurred.

5. Units damaged.

6. Names of Lowest Replaceable Units (LPU) damaged by lightning and replaced.

7. Names of replacement parts installed due to the lightning damage. Differentiate, if you can, between other types of damage and the lightning-related damage.

8. Estimated cost of lightning-damaged parts[3]

9. Estimated cost of labor to bring station back on-line.

---

[1] A technician of the WSR-88D site should fill in this part of the Web page as soon as the circumstances of lightning strike occurrence and damage are known. OSF will complete the part of the page devoted to the analysis of the lightning damage, after which the finished Web page is converted into a hard-copy document available to any potential user.

[2] The following information about a given site can be "hardwired," using the name of the station only: (1) Latitude and Longitude of the station, (2) Elevation of the site, (3) Category of radar tower according to its height, (4) Category of the station according to RDA-RPG connection and the type of communication link to WFO, and (5) Type of lightning protection on a radome.

[3] The price list should be made available to site personnel.

10. Estimated time-loss due to damage.

11. Specific questions related to effects of lightning:

11a. Did you or any of your co-workers see or hear the lightning occur? What type of thunder did you hear (explosion, crackling noise, or low frequency rumble)? If so, what part of the radar did it strike, or if it was a nearby strike, how far away did it hit (estimate), and what physical object did it appear to hit?

11b. In your investigation, what evidence of a lightning hit or types of damage did you or any of your co-workers find (burn marks, burned wires, popped circuit breakers, etc.)?

11c. If it was a nearby strike which contacted the ground, did you or any of your co-workers see any evidence of channeling in the ground toward the radar?

11d. Describe all physical evidence that indicates that lightning either struck the radar equipment or a nearby ground structure, and thus caused damage.

Inputs to points 12-16 should be provided by OSF following analysis of the answers to the previous questions.

12. Was a thunderstorm overhead or near the station during the time when the lightning-related damage occurred?

13. Did a lightning flash to ground occur at the time of the reported damage?

14. What was the estimated distance to the strike point from the station? Was the lightning damage caused by a direct, or nearby strike?

15. If damage was caused by a direct lightning strike, where is the most likely point of entry on the installation?

16. Did nearby utility power fixtures or communication lines channel the strike into the radar site?

Indication that the given case of lightning damage has been analyzed should be posted at the end of this Web page. The OSF summary should contain a description of the lightning path (if possible to determine) from the point of entrance, an interpretation of observations during the time of damage, etc., and recommendations, if any, for changes in the lightning protection system at the WSR-88D site.

Appendix: Leader Potential and Electric Field Change

Introduction

The potential of the lightning leader is the one variable instrumental in deriving the main characteristics of the leader process, such as leader charges, channel diameter, and charge per unit length. The leader's potential is determined by the ambient potential distribution in the cloud region penetrated by the leader [e.g., Mazur and Ruhnke, 1998]. The leader's potential is also the dominant factor affecting leader interaction with a ground structure, including the maximum length of the final "jump-over" toward the structure, as demonstrated by Mazur et al.[2000], with a computer-simulated modeling of leader interaction with a tall mast. We propose a method of deriving the leader potential from measurements of electric field changes produced by cloud-to-ground flashes. Previously, leader potential values have been estimated only empirically.

We define the analytical relationship between leader potential and E-field change during the return stroke process in cloud-to-ground (CG) flashes by following the derivations in [2], based on the bi-directional uncharged leader concept. A leader, after initiation at a location of high electric field in a cloud, will assume the potential ϕ that can be determined by integration of the ambient electric potential distribution $\phi(z)$ over a length L of the leader channel.

$$\phi = \frac{1}{L} \int_{o}^{L} \phi(z) dz \tag{1}$$

While the total charge of the leader is zero before touching the ground, the leader potential shifts from ϕ to zero upon contact with the ground. This shift of potential is equivalent to the effect of a transfer of charge, Q, with a constant charge per unit length, q, along the leader channel during the return stroke process. Therefore, the charge per unit length, q, deposited by the return stroke in the leader channel of capacitance per unit length, c, is:

$$q = - c \phi \tag{2}$$

The capacitance, C, of the leader channel, that can be approximated as a vertical, thin, long conductor over the ground (with diameter d and length Z), is calculated using this formula in [3]:

$$c = 2\pi\varepsilon / ln(L/d) \tag{3}$$

The electric field change ΔE on the ground produced at distance D by the return stroke process is:

$$\Delta E = - q/(2\pi\varepsilon) * [1/D-1/(D^2 + Z^2)^{1/2}] \quad (4)$$

Using equations (2) and (3) one arrives at:

$$\Delta E = \phi/ln(L/d) * [1/D-1/(D^2 + Z^2)^{1/2}] \quad (5)$$

The unknown variables in these equations are the distance from the sensor to the leader, D, and the vertical extension of the channel, Z. ΔE is measured at various distances from a lightning strike by several "slow antenna" sensors. Variables q, D and Z are obtained by solving a system of equation (4). In order to determine the leader potential ϕ, we need also to assume the effective diameter, d, of the leader channel.

The relationship between the diameter of the channel and its charges is based on the assumption that the charges are distributed in a corona sheath around the current-carrying core of the channel. The maximum radial E-fields in this region do not exceed the electrical breakdown E-field of 3 MV m^{-1}. Thus, the diameter of the charge-carrying channel, d, is:

$$d = q/\pi\varepsilon 3x10^6 \qquad [m] \quad (6)$$

The diameter we use in calculating the leader's potential in equation (5) is the average diameter of the channel during the return stroke process. The estimated length of the last negative leader step, L, is a function of the leader potential ϕ, in kV, and the constant electric field along the negative streamer that is 750 kV m^{-1} [5]:

$$L_{st} = \phi/750 \quad [m] \quad [7]$$

We postulate that the last step of the downward stepped leader is longer, or equal to, the "striking distance" to the ground structure, which would be the actual length of the last step.

Measurements

Assuming that the location of the return stroke channel is known from the NLDN, we need a minimum of two slow antenna stations to obtain the channel length, Z, and the total charge, Q, of the return stroke process, using equation (4). To demonstrate the feasibility of determining the leader's potential experimentally, we analyzed the E-field changes of CG flashes in a modest convective storm in Florida, on 9 August 2000. Records showing good resolution of E-field records were obtained with two stations separated by 6 km when CG flashes were less than 20 km away from each station. The instruments we used in our field measurements were a GPS -synchronized slow antenna system (a 10-m long horizontal wire antenna, suspended about 1m above the ground, and a

high-pass amplifier with the time constant of 0.5 s), and a PC, with a 12-bit A/D converter. The converter's time resolution of 200 μs allowed us to identify the beginning and the end of the return stroke in the E-field change record. GPS synchronization allowed us to find matching records from the same flash at two stations and on the NLDN listing. A total of 25 CG flashes were recorded. For calculations of the leader potential, we used only the voltage change that corresponded to the first return stroke.

The calculated values of leader potential are generally in the range of 30 -130 MV, close to the range of 20-100 MV predicted by Berger [in 4]. The peak current data provided by the NLDN network indicate that the CG flashes in this storm were of a current magnitude below average values. A plot of the leader potential values derived from the electric field changes during the return strokes, versus the peak values of the first return stroke current, from the NLDN data (see Fig. 1), shows a weak correlation between them with a correlation coefficient of 0.68.

Table 1. Tabulation of measured and calculated characteristics of first stepped leaders in CG flashes

	D to St. #1	*D* to St. #2	*E* St. #1	*E* St. #2	*Z*	*q*	*Q*	ϕ	*L*	RS current
#	(km)	(km)	(V m^{-1})	(V m^{-1})	(m)	(mC m^{-1})	(C)	(MV)	(m)	(kA)
1	20.29	15.06	40.78	81.39	15230	0.23	3.50	35.6	47	12
2	19.25	14.38	47.50	106.88	6696	0.92	6.14	105.6	141	15
3	21.68	16.72	52.84	99.70	14140	0.39	5.56	56.5	75	25
4	20.86	17.06	35.61	63.05	6314	0.96	6.09	109.2	146	18
5	19.44	14.48	22.45	47.35	10880	0.19	2.08	29.0	39	9
6	16.51	11.03	53.07	131.75	12700	0.24	2.99	35.5	47	10
7	17.36	12.05	63.48	166.25	7962	0.67	5.37	83.5	111	12
8	23.64	19.39	33.90	56.43	13170	0.35	1.65	51.0	68	11
9	15.51	10.82	70.06	170.79	9176	0.43	3.98	58.3	78	7
10	17.41	12.42	69.60	150.64	13330	0.33	4.36	47.8	64	11
11	17.24	12.90	45.54	97.75	8235	0.45	3.69	59.0	79	15
12	16.47	12.26	50.57	103.16	5954	0.70	4.18	82.7	110	9
13	11.39	7.53	127.04	294.16	11410	0.27	3.13	40.2	54	13
14	18.63	14.15	40.48	80.52	11180	0.29	3.29	42.7	57	11
15	20.95	16.57	59.86	108.32	12230	0.51	6.26	69.8	93	20
16	21.70	17.50	30.11	52.64	11420	0.32	3.61	45.5	61	9
17	18.21	14.14	35.61	68.70	9500	0.32	3.03	44.7	60	13
18	11.74	8.32	121.99	290.46	6577	0.62	4.11	76.1	101	20
19	12.37	9.17	166.89	331.66	9580	0.55	5.26	71.8	96	25
20	15.51	11.37	70.42	156.51	8119	0.53	4.33	68.4	91	19
21	10.32	4.69	316.83	1260.20	12260	0.51	6.27	69.9	93	15
22	16.22	11.06	42.55	111.73	8847	0.31	2.78	43.9	58	10
23	18.63	16.91	79.07	104.93	3356	5.17	17.36	371.0	495	32
24	24.30	18.24	24.97	49.81	16280	0.20	3.25	31.6	42	5
25	19.55	15.95	46.34	81.54	7135	0.83	5.93	98.2	131	16

An error analysis showed that the two-station system is only minimally suitable to obtain data on leader characteristics. For flashes with a distance differential to the stations of less than 3 km, it becomes essential that the locations of the flash be known with an accuracy of within 100 m. Therefore, for greater accuracy in estimating the leader's characteristics, it would be advisable to use four or more slow antenna stations for data acquisition, and also to determine lightning locations from the electric field measurements. (The NLDN can be used to confirm these flashes).

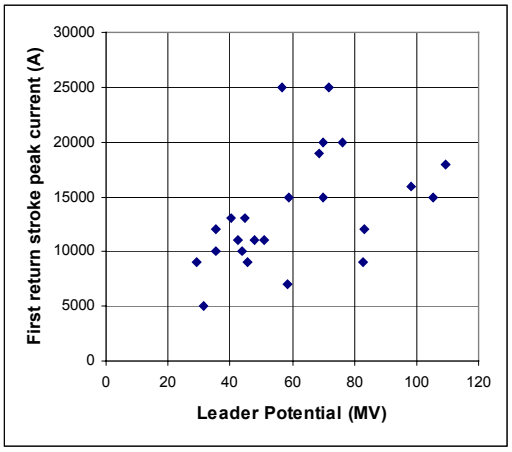

Figure 29. Correlation between return stroke current and leader potential.

Conclusion

The proposed remote method of evaluating leader potential using measurements of electric field changes produced by cloud-to-ground lightning allows us, with relative ease, to obtain significant statistical data on lightning leader potentials and, therefore, the range of step length in negative leaders in any geographical region. In present practice, direct measurements of return stroke currents, for relating to the "striking distance," are much more complex, require a tall structure, and produce rather small amounts of data. In addition, using leader potential rather than return stroke current makes more physical sense for evaluation of the dimensions of leader steps in their progression towards a grounded structure.

Admittedly, the proposed method of evaluation of leader potential is based on several modeling assumptions. Therefore, validation of the model requires comparison of some leader characteristics calculated using our method with those obtained from observations with independent measuring systems, e.g., a lightning mapping system.

References

[1] Mazur, V., L.H. Ruhnke, A. Bondiou-Clergerie, and P. Lalande, Computer simulation of a downward negative stepped leader and its interaction with a ground structure, J. Geophys. Res.,105, 22,361-22,369, 2000.

[2] Mazur, V., L. H. Ruhnke, P. Laroche, The relationship of leader and return stroke processes in cloud-to-ground lightning, Geophys. Res. Letters., 22, 2613-2616, 1995.

[3] Meinke, H., and F.W. Gundlach, Taschenbuch der Hochfrequenztechnik, p.52, Springer-Verlag, New York, 1956.

[4] Golde, R. H., Lightning (vol.2, Lightning Protection), Academic Press, New York, 1977.

[5] Bacchiega, G. L., A. Gazzani, M. Bernardi, I. Gallimberti, A. Bondiou, Theoretical modeling of the laboratory negative stepped leader, 1994 International Aerospace and Ground Conf. on Lightning and Static Electricity, Mannheim (Germany), May 24-27, 1994.

Publication and Presentations Related to Work on the MOU

Journal articles

Mazur, V., and L. H. Ruhnke, Computer simulation of a downward negative stepped leader and its interaction with a ground structure, J. Geophys. Res., 105, 22,361-22,369, 2000.

Mazur, V., and L. H. Ruhnke, Modeling the interaction between downward negative leaders and radar antenna towers, submitted to IEEE Trans. on EMC.

Mazur, V., and L. H. Ruhnke, Determining leader potential in cloud-to-ground flashes, submitted for publication to J. Geophys. Res. Atmospheres.

Presentations

Mazur, V. Contemporary understanding of physics of lightning and its application to lightning protection, International Conference on Grounding and Earthing, Belo Horizonte, Brazil, June 18-21, 2000.

Mazur, V. and L. H. Ruhnke, Lightning magnitude and protection properties of air terminals, Proc. 25th International Conference on Lightning Protection, Rhodes, Greece, 18-22 September 2000, pp. 318-322.

Mazur, V. and L. H. Ruhnke, Computer simulation of a downward negative stepped leader, Proc. 11th International Conference on Atmospheric Electricity, Guntersville, Alabama, June 7-11, 1999, pp. 26-29.

Mazur, V. and L. H. Ruhnke, Modeling of lightning protection provided for a building by a mast, Proc. International Conference of Grounding and Earthing, Belo Horizonte, Brazil, April 12-16, 1998.

Acknowledgements. We are grateful to the following colleagues from NSSL: to Dennis Nealsen and Richard Wahkinney for their help with the manufacturing of the various parts of the field observational and measurement system; to Dennis Nealsen and Dan Major for their assistance in running the field program; and to Doug Kennedy for his invaluable help with setting up the data acquisition software. Tony Harper from WSR-88D in Ruskin, FL was a generous host who provided us with all the help we needed to set up and monitor our observational system there. Finally, the authors of this report are most grateful to Marijo Hennagin-Mazur for her immeasurable assistance with editing.